

774

OGLE
OPTICAL GRAVITATIONAL LENSING EXP.

GA - 21A

No New I.D. Recorded

Table of Contents

1. Introduction
2. Errata/Change Log
3. LINKS TO RELEVANT INFORMATION IN THE ONLINE NSSDC INFORMATION SYSTEM
4. Catalog Materials
 - a. Associated Documents
 - b. Core Catalog Materials

1. INTRODUCTION:

The documentation for this data set was originally on paper, kept in NSSDC's Data Set Catalogs (DSCs). The paper documentation in the Data Set Catalogs have been made into digital images, and then collected into a single PDF file for each Data Set Catalog. The inventory information in these DSCs is current as of July 1, 2004. This inventory information is now no longer maintained in the DSCs, but is now managed in the inventory part of the NSSDC information system. The information existing in the DSCs is now not needed for locating the data files, but we did not remove that inventory information.

The offline tape datasets have now been migrated from the original magnetic tape to Archival Information Packages (AIP's).

A prior restoration may have been done on data sets, if a requestor of this data set has questions; they should send an inquiry to the request office to see if additional information exists.

2. ERRATA/CHANGE LOG:

NOTE: Changes are made in a text box, and will show up that way when displayed on screen with a PDF reader.

When printing, special settings may be required to make the text box appear on the printed output.

Version	Date	Person	Page	Description of Change
01				
02				

3 LINKS TO RELEVANT INFORMATION IN THE ONLINE NSSDC INFORMATION SYSTEM:

<http://nssdc.gsfc.nasa.gov/nmc/>

[NOTE: This link will take you to the main page of the NSSDC Master Catalog. There you will be able to perform searches to find additional information]

4. CATALOG MATERIALS:

- a. Associated Documents To find associated documents you will need to know the document ID number and then click here.
<http://nssdcftp.gsfc.nasa.gov/miscellaneous/documents/>

- b. Core Catalog Materials

GA - 21A

OPTICAL GRAVITATIONAL LENSING EXPERIMENT

GA - 21A

No New I.D. Recorded

This data set consists of 15 magnetic 8mm tapes written in binary. The tapes were created on the VAX computer. The D and C numbers along with the number of files and timespans are as follows:

D#	C#	FILES	TIME SPAN
D-108216	C-032346	4	04/13/92 - 04/20/92
D-108222	C-032352	3	04/13/93 - 04/20/92
D-108221	C-032351	4	04/13/92 - 05/08/92
D-108217	C-032347	6	05/06/92 - 05/17/92
D-108223	C-032353	8	05/07/92 - 05/31/92
D-108218	C-032348	4	05/29/92 - 06/04/92
D-108224	C-032354	4	05/30/92 - 06/30/92
D-108219	C-032349	2	06/30/92 - 07/03/92
D-108225	C-032355	23	06/30/92 - 07/08/92
D-108226	C-032356	10	07/08/92 - 07/10/92
D-108220	C-032350	3	07/15/92 - 08/10/92
D-108227	C-032357	17	07/16/92 - 07/27/72
D-108228	C-032358	17	07/21/92 - 07/30/92
D-108229	C-032359	7	07/29/92 - 08/06/92
D-108230	C-032360	6	08/10/92 - 08/11/92

From: NCF::KEMPER "Ed Kemper (301)286-3431" 26-OCT-1993 13:18:02.78
To: POST
CC: KEMPER
Subject: Possible ingest script for OGLE data

Ingest Script for OGLE

Ed Kemper x3431

Tape	Files	
OGLE1	skip 1 copy 2-4	<i>re-do Done</i>
OGLE2	copy 1-6	<i>Done</i>
OGLE3	copy 1-4	<i>DONE</i>
OGLE4	copy 1-2	<i>DONE</i>
OGLE5	copy 1-3	<i>DONE</i>
OGLE6	copy 1-4	<i>DONE</i>
OGLE7	copy 1-2 skip 3	<i>RE-DO Done</i>
OGLE8	skip 1 copy 2-7 skip 8	<i>Done</i>
OGLE9	copy 1 skip 2 copy 3-4	<i>Done</i>
OGLE10	copy 1-21 skip 22-23	<i>DONE</i>
OGLE11	copy 1-2 skip 3 copy 4-10	<i>DONE</i>
OGLE12	copy 1-16 skip 17	<i>DONE</i>
OGLE13	copy 1-17	<i>Done</i>
OGLE14	copy 1-7	<i>Done</i>
OGLE15	skip 1-3 copy 4-6	<i>Done</i>

The Optical Gravitational Lensing Experiment

by

A. Udalski, M. Szymański, J. Kałużny, M. Kubiak
Warsaw University Observatory, Al. Ujazdowskie 4, 00-478 Warszawa, Poland

and

Mario Mateo¹

The Observatories of the Carnegie Institution of Washington, 813 Santa Barbara Street,
Pasadena, CA 91101 USA

Received October 31, 1992

ABSTRACT

The technical features and initial results of the first observing season of the long term project called the Optical Gravitational Lensing Experiment are described. The ultimate aim of this project is to detect a statistically significant number of gravitational microlensing events in the direction of the Galactic Bulge. We discuss our planned future enhancements to the experiment that will allow us to achieve this goal.

1. Introduction

There is growing evidence that galaxies are embedded in large, massive halos consisting of unseen dark matter. Paczyński (1986) and Griest (1991) found that if the massive Galactic halo is made of massive compact objects (black holes, brown dwarfs, *etc.*) then any star in LMC or SMC has a probability of about 10^{-6} of being "strongly" gravitationally micro-lensed, *i.e.* its apparent luminosity would be increased by at least 0.34 magnitude (throughout this paper we shall refer to any gravitational amplification larger than this amplitude as an "event" unless otherwise stated). The same phenomenon will also operate on stars in the Galactic Bulge (Paczynski 1991, Griest *et al.* 1991). Moreover, Bulge stars are subject to lensing by an additional source that is known to exist. Specifically, a star in Baade's

¹ Hubble Fellow

Window has a probability of about 4×10^{-7} of being strongly micro-lensed by an ordinary Galactic Disk star. This lensing probability decreases with increasing Galactic latitude, dropping to 2.5, 1.7, and 1.1×10^{-7} at $|b| = 6^\circ$, 8° , and 10° , respectively, for a reasonable model describing the distribution of matter in the Galactic Disk. If there is as much matter in brown dwarfs as in main sequence stars in the Galactic disk, then these probabilities should be doubled. The durations of events scales as $t \sim 1 \text{ month } (M_{\text{lens}}/M_\odot)^{-1/2}$ (Paczynski 1991); for a lens of one Jupiter mass, the event duration is about one day, depending also on the relative distances of the lens and source.

The main practical difficulty in detecting micro-lensing events is the necessity of photometrically monitoring millions of stars over a long period of time in order to detect a significant number of isolated events. On the other hand many interesting "side" projects may be carried out simultaneously using the data generated by such a survey. For example, Baade's Window contains a significant number of Algol variables (Gaposchkin 1954). These stars can be used to obtain an independent estimate of the turnoff mass and the age of the Bulge by deriving a complete Algol luminosity function (Preston 1992). Another interesting issue is presence of a bar in the Galactic center (Blitz and Spergel 1991). From samples of RR Lyr stars located symmetrically about the Galactic Center, accurate reddenings can be derived and new information on the Bulge structure along our line-of-sight can be obtained using the data from a multi-color lensing survey. Finally, by combining many images of a single survey field, deep color-magnitude diagrams can be constructed, providing information on the age distribution and relative numbers of different types of stars throughout the Bulge.

In April 1992 we started a long term observational project called the Optical Gravitational Lensing Experiment (OGLE). The ultimate aim of this project is to detect a statistically significant number of microlensing events towards the Galactic Bulge. The 1992 observations represent a pilot micro-lensing survey of the Bulge designed to test our ability to monitor millions of stars over a long period of time. In this paper we describe the technical features of this project, as well as some preliminary results obtained in the 1992 Bulge season and a description of our future plans (see also Udalski *et al.* 1992 for a brief description of the project).

2. Observations

A total of 51 nights were formally allocated on the 1m Swope telescope of the Las Campanas Observatory, operated by the Carnegie Institution of Washington. During the observing season, an additional 14 open nights were obtained for this project, resulting in a total of 65 nights from 12 April 1992 through 10 August 1992. The allotted time was split into six separate "subruns" lasting from 6 to 15 days, usually during grey or bright time. All of the observations were obtained using a single Ford (Loral) 2048×2048 CCD as the detector. The main reason

for selection of this chip was its pixel size – $15 \mu\text{m}$ (resulting in a scale of $0.44 \text{ arcsec/pixel}$) – ensuring good resolution of the dense Bulge fields and adequate sampling of the stellar images. The full frame covered an area of $15 \times 15 \text{ arcmin}$ on the sky. The readout noise of the chip was $12 e^-$ for a gain set at $3.4 e^-/\text{DN}$.

The primary target of our pilot program was the Galactic Bulge. Fourteen separate CCD fields located in four distinct regions of the Bulge were observed throughout the entire run. These included nine CCD fields covering a $40 \times 40 \text{ arcmin}$ area centered on Baade's Window (this covers practically the whole area of this window), one CCD field at $b = -8^\circ$ (Temdrup 1988), and four CCD fields to study the structure of the "Galactic Bar" located in two regions placed symmetrically on either side of the Galactic Center ($l \approx \pm 5^\circ$ and $b \approx -3^\circ$). A small number of frames were also obtained in the Bulge window described by Blanco (1992). Table 1 lists the coordinates and our acronyms of all fields observed during the 1992 season. Adjacent CCD fields in Baade's Window and the "Galactic Bar" fields overlap by approximately 1 arcmin in order to facilitate calibration to a common photometric and astrometric system. Fig. 1 is a reproduction of a mosaic of the nine CCD fields making up our coverage of Baade's Window and the four CCD fields making up the two "Galactic Bar" regions we observed.

Table 1
Galactic Bulge Fields.

Field	RA (2000.0)	Dec (2000.0)	Remarks
BW1	$18^{\text{h}}02^{\text{m}}24^{\text{s}}$	$-29^\circ 49' 05''$	Baade's Window #1
BW2	$18^{\text{h}}02^{\text{m}}24^{\text{s}}$	$-30^\circ 15' 05''$	Baade's Window #2
BW3	$18^{\text{h}}04^{\text{m}}24^{\text{s}}$	$-30^\circ 15' 05''$	Baade's Window #3
BW4	$18^{\text{h}}04^{\text{m}}24^{\text{s}}$	$-29^\circ 49' 05''$	Baade's Window #4
BW5	$18^{\text{h}}02^{\text{m}}24^{\text{s}}$	$-30^\circ 02' 05''$	Baade's Window #5
BW6	$18^{\text{h}}03^{\text{m}}24^{\text{s}}$	$-30^\circ 15' 05''$	Baade's Window #6
BW7	$18^{\text{h}}04^{\text{m}}24^{\text{s}}$	$-30^\circ 02' 05''$	Baade's Window #7
BW8	$18^{\text{h}}03^{\text{m}}24^{\text{s}}$	$-29^\circ 49' 05''$	Baade's Window #8
BWC	$18^{\text{h}}03^{\text{m}}24^{\text{s}}$	$-30^\circ 02' 00''$	Baade's Window Center
TP8	$18^{\text{h}}17^{\text{m}}55^{\text{s}}$	$-32^\circ 54' 00''$	Temdrup Field $b = -8^\circ$
MMS-A	$17^{\text{h}}47^{\text{m}}30^{\text{s}}$	$-34^\circ 45' 00''$	Galactic Bar Field
MMS-B	$17^{\text{h}}47^{\text{m}}30^{\text{s}}$	$-34^\circ 57' 00''$	Galactic Bar Field
MM7-A	$18^{\text{h}}10^{\text{m}}53^{\text{s}}$	$-25^\circ 54' 20''$	Galactic Bar Field
MM7-B	$18^{\text{h}}11^{\text{m}}47^{\text{s}}$	$-25^\circ 54' 20''$	Galactic Bar Field
BL1-A	$18^{\text{h}}08^{\text{m}}29^{\text{s}}$	$-31^\circ 09' 35''$	Blanco 1 Field
BL1-B	$18^{\text{h}}09^{\text{m}}29^{\text{s}}$	$-31^\circ 09' 35''$	Blanco 1 Field

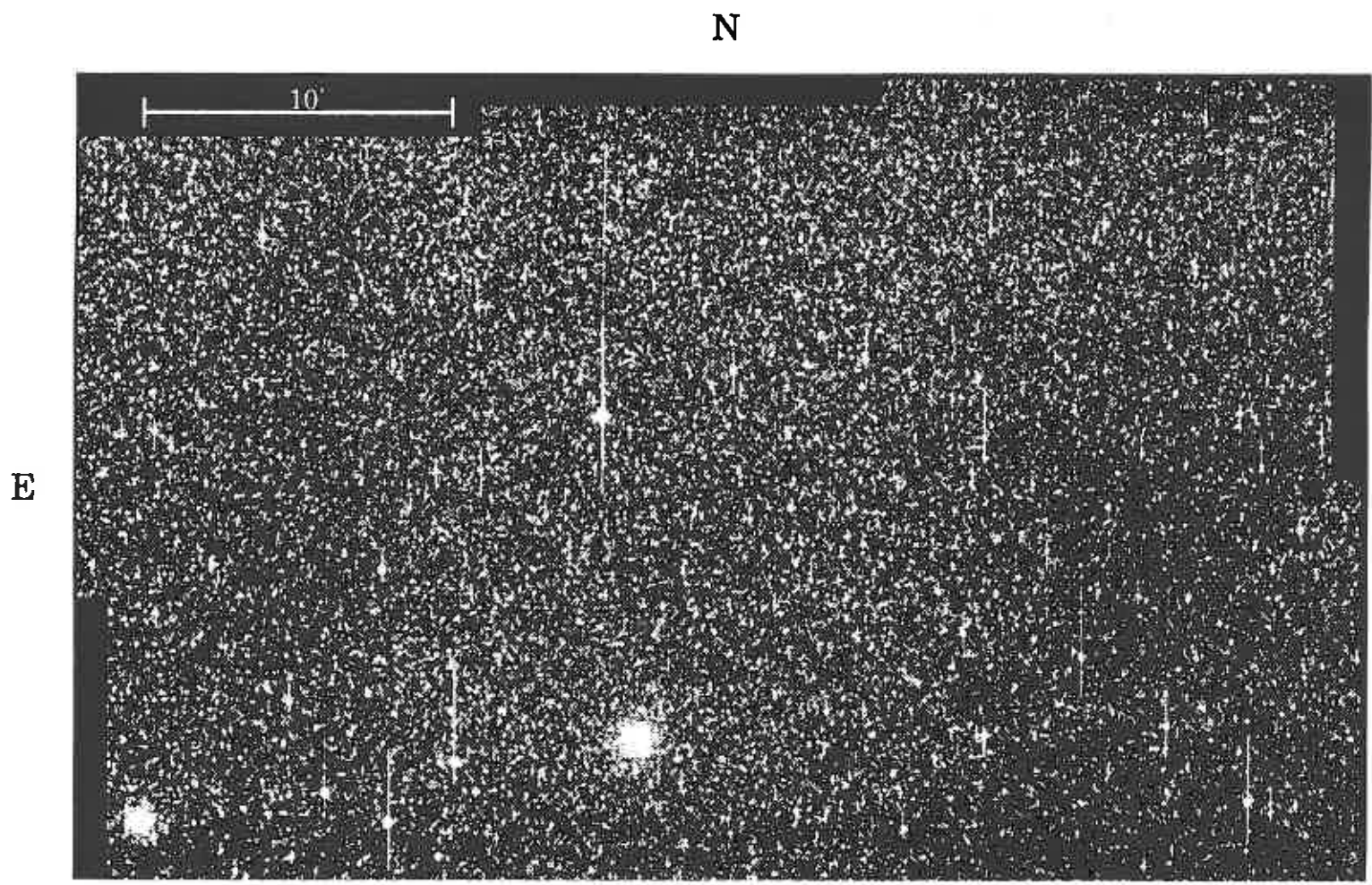


Fig. 1a. Northern part of the Baade's Window. Two characteristic globular clusters are NGC 6528 (left) and NGC 6522.

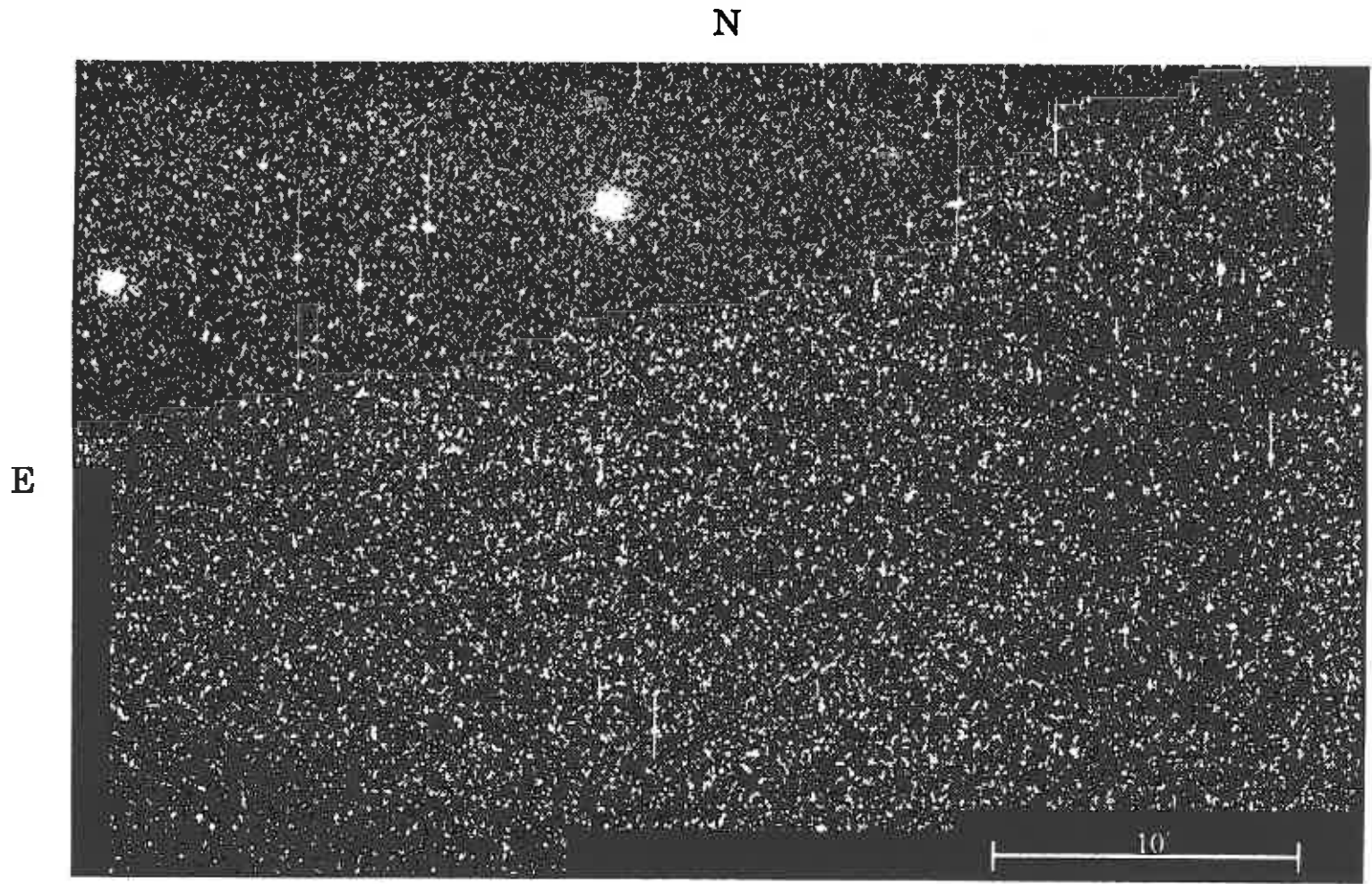


Fig. 1b. Southern part of the Baade's Window. Two characteristic globular clusters are NGC 6528 (left) and NGC 6522.

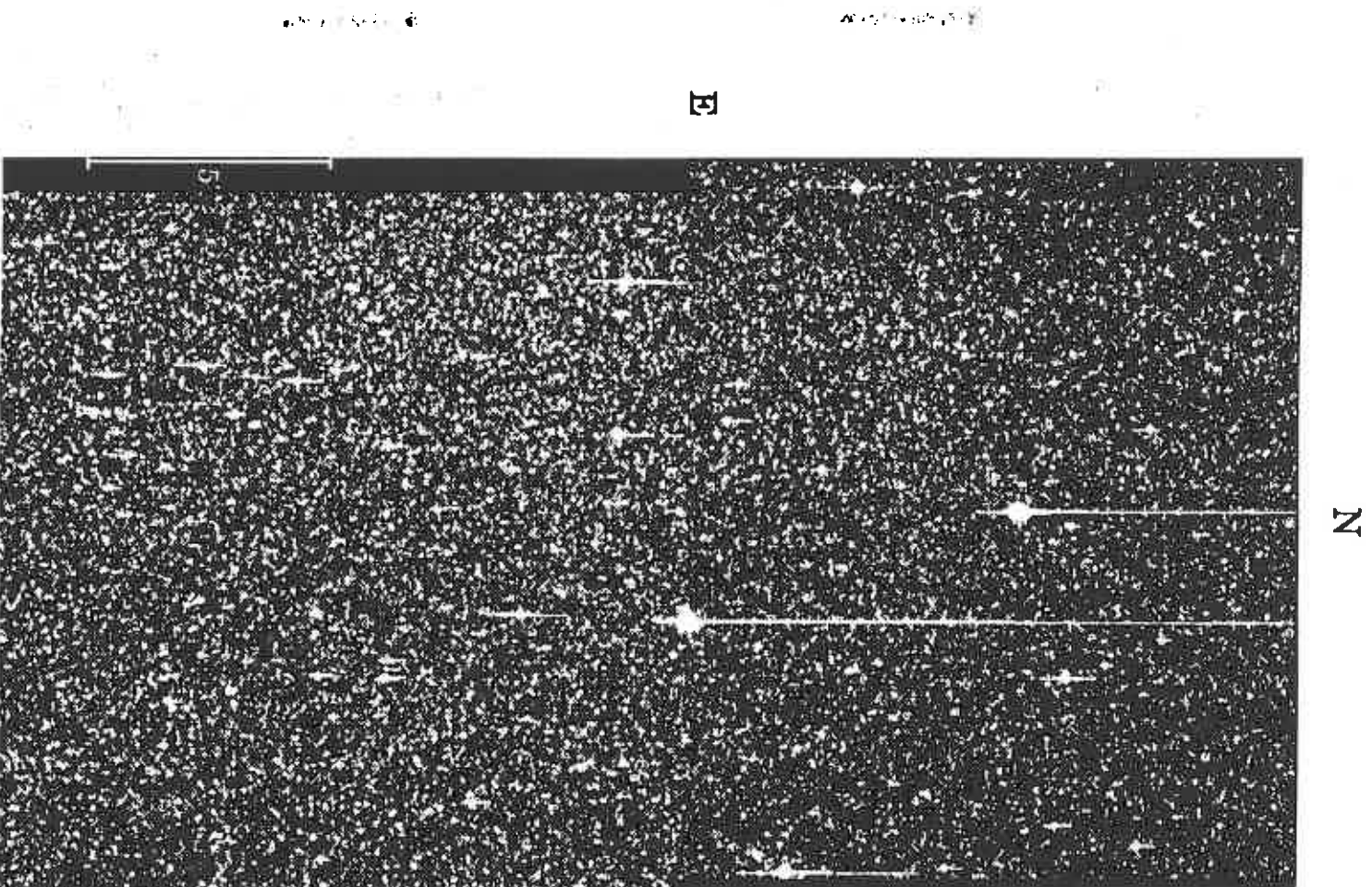


Fig. 1c. The "Galactic Bar" field MMS ($l \approx 5^\circ$, $b \approx -3^\circ$).

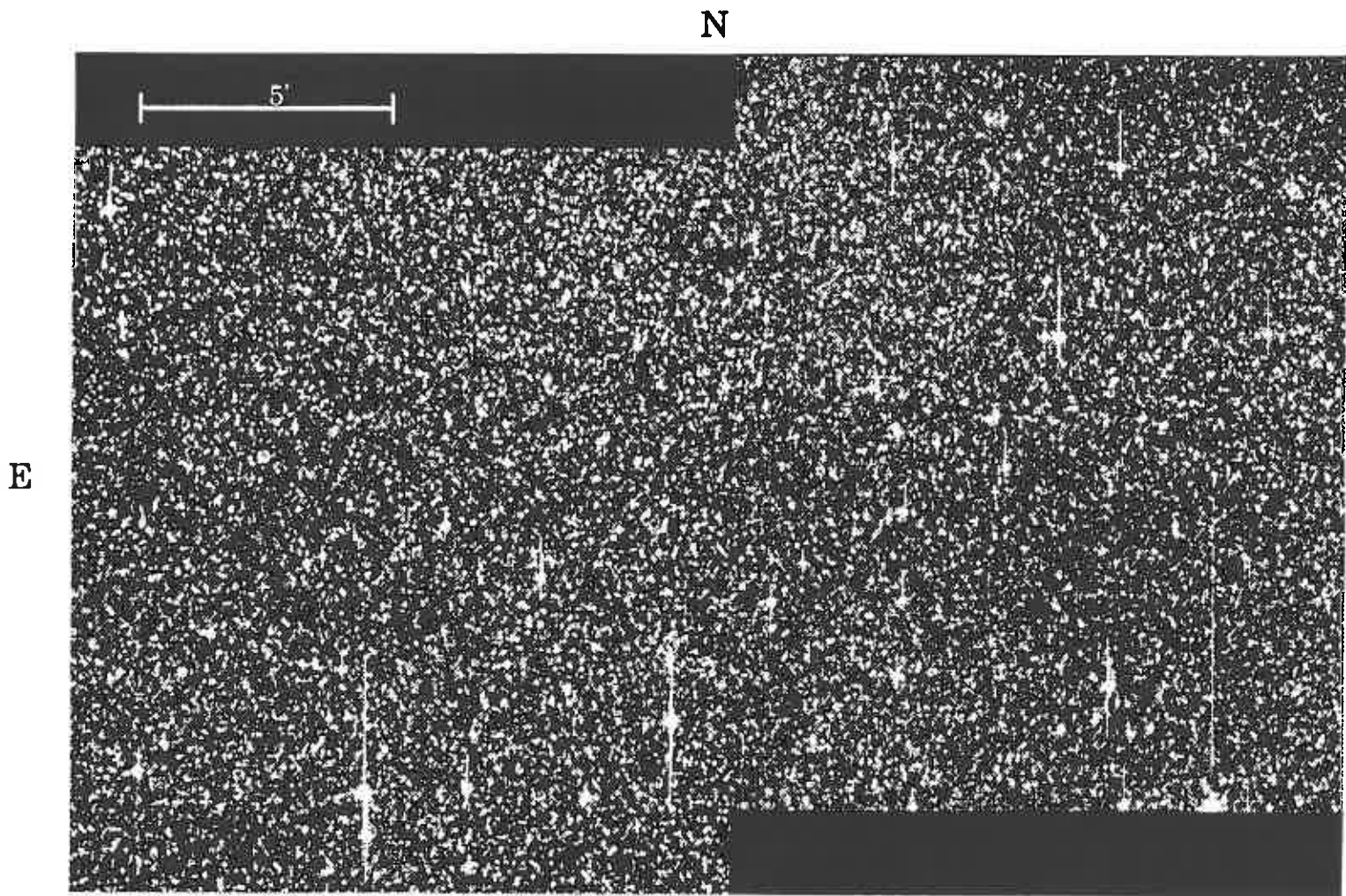


Fig. 1d. The "Galactic Bar" field MM7 ($l \approx -5^\circ$, $b \approx -3^\circ$).

Table 2
Observed Clusters of Galaxies.

Abell Number (+ subfield)	R.A. (2000.0)	Dec (2000.0)	No of V Obs.	No of I Obs.
2717	0 ^h 03 ^m 15 ^s	-35°57'30"	5	2
2933	1 ^h 40 ^m 42 ^s	-54°33'45"	6	1
2995	2 ^h 15 ^m 10 ^s	-24°49'55"	6	1
754-1	9 ^h 08 ^m 22 ^s	-9°39'10"	8	0
754-2	9 ^h 09 ^m 12 ^s	-9°39'10"	8	0
930	10 ^h 06 ^m 54 ^s	-5°38'35"	8	0
957	10 ^h 13 ^m 57 ^s	-0°54'50"	9	0
970	10 ^h 17 ^m 33 ^s	-10°42'00"	9	0
979	10 ^h 20 ^m 23 ^s	-7°54'05"	9	0
993	10 ^h 21 ^m 55 ^s	-4°58'05"	7	0
1020	10 ^h 27 ^m 50 ^s	10°24'45"	7	0
1060	10 ^h 36 ^m 50 ^s	-27°31'30"	13	0
1139	10 ^h 58 ^m 03 ^s	1°31'00"	9	0
1216	11 ^h 17 ^m 43 ^s	-4°28'15"	8	0
3490	11 ^h 45 ^m 17 ^s	-34°26'30"	8	1
3505	12 ^h 08 ^m 39 ^s	-34°26'30"	11	0
3528	12 ^h 54 ^m 16 ^s	-29°01'05"	10	1
1631	12 ^h 52 ^m 49 ^s	-15°26'15"	7	1
1644	12 ^h 57 ^m 14 ^s	-17°22'10"	8	1
3545	13 ^h 11 ^m 21 ^s	-34°04'45"	9	1
3549	13 ^h 14 ^m 20 ^s	-29°26'45"	9	1
1709	13 ^h 18 ^m 41 ^s	-21°27'40"	8	1
1736	13 ^h 26 ^m 52 ^s	-27°07'30"	8	1
3558-1	13 ^h 27 ^m 20 ^s	-31°22'20"	10	1
3558-2	13 ^h 28 ^m 25 ^s	-31°22'20"	9	1
3558-3	13 ^h 27 ^m 20 ^s	-31°36'20"	9	1
3558-4	13 ^h 28 ^m 25 ^s	-31°36'20"	9	1
3559-1	13 ^h 29 ^m 25 ^s	-29°24'20"	9	1
3559-2	13 ^h 29 ^m 25 ^s	-29°38'20"	8	1
3559-3	13 ^h 30 ^m 25 ^s	-29°24'20"	8	1
3559-4	13 ^h 30 ^m 25 ^s	-29°38'20"	8	1

Table 2
concluded

Abell Number (+ subfield)	R.A. (2000.0)	Dec (2000.0)	No of V Obs.	No of I Obs.
3562-1	13 ^h 32 ^m 55 ^s	-31°40'15"	11	1
3562-2	13 ^h 34 ^m 00 ^s	-31°40'15"	12	1
3566-1	13 ^h 38 ^m 26 ^s	-35°33'05"	8	1
3566-2	13 ^h 39 ^m 26 ^s	-35°33'05"	8	1
3570	13 ^h 46 ^m 49 ^s	-37°54'50"	9	1
3571-1	13 ^h 46 ^m 56 ^s	-32°51'50"	9	1
3571-2	13 ^h 47 ^m 56 ^s	-32°51'50"	8	1
3577-1	13 ^h 53 ^m 46 ^s	-27°50'35"	7	1
3577-2	13 ^h 54 ^m 46 ^s	-27°50'35"	7	1
1837	14 ^h 01 ^m 45 ^s	-11°10'20"	6	0
2052	15 ^h 16 ^m 44 ^s	7°01'05"	6	0
2063	15 ^h 23 ^m 01 ^s	8°38'25"	4	0
3651	19 ^h 52 ^m 01 ^s	-55°09'20"	5	1
3667	20 ^h 12 ^m 28 ^s	-56°49'05"	6	3
3677	20 ^h 26 ^m 19 ^s	-33°21'15"	6	2
3703	20 ^h 40 ^m 00 ^s	-61°20'30"	5	2
3716	20 ^h 59 ^m 30 ^s	-52°42'50"	6	2
3733	21 ^h 01 ^m 57 ^s	-28°03'15"	6	2
3806	21 ^h 46 ^m 36 ^s	-57°17'15"	6	2
3806-2	21 ^h 46 ^m 39 ^s	-57°02'25"	4	2
3806-3	21 ^h 46 ^m 39 ^s	-57°30'25"	4	2
2382	21 ^h 52 ^m 01 ^s	-15°39'00"	7	1
3822	21 ^h 54 ^m 04 ^s	-57°51'00"	7	1
3825	21 ^h 58 ^m 20 ^s	-60°23'50"	5	1
2399	21 ^h 57 ^m 31 ^s	-7°47'50"	6	1
3826	21 ^h 59 ^m 53 ^s	-56°09'45"	5	1
2657	23 ^h 44 ^m 51 ^s	9°08'30"	6	1
4038-1	23 ^h 47 ^m 40 ^s	-28°04'00"	5	2
4038-2	23 ^h 47 ^m 40 ^s	-28°15'30"	7	2
2670	23 ^h 54 ^m 10 ^s	-10°24'30"	7	1
4059	23 ^h 56 ^m 40 ^s	-34°40'30"	8	2

Table 3
Log of Cluster of Galaxies Observations.

Frame No	Date	UT - Middle of exp.	Abell Number	Filter
1000	13 Apr 92	3.3167	3490	V
1001	13 Apr 92	3.6411	3505	V
1002	13 Apr 92	3.9647	3528	V
1003	13 Apr 92	4.2900	3562-1	V
1004	13 Apr 92	4.5416	3562-2	V
1005	13 Apr 92	4.8136	3558-1	V
1006	13 Apr 92	5.0519	3558-2	V
1007	13 Apr 92	5.3242	3558-3	V
1008	13 Apr 92	5.5711	3558-4	V
1027	14 Apr 92	2.9822	1060	V
1028	14 Apr 92	3.3717	3559-1	V
1029	14 Apr 92	3.7908	3559-2	V
1030	14 Apr 92	4.0694	3559-3	V
1031	14 Apr 92	4.3125	3559-4	V
1032	14 Apr 92	4.6900	3566-1	V
1033	14 Apr 92	5.0314	3566-2	V
1034	14 Apr 92	5.2769	3571-1	V
1035	14 Apr 92	5.5908	3571-2	V
1036	14 Apr 92	5.9228	2052	V
1055	15 Apr 92	0.2067	754-1	V
1056	15 Apr 92	0.5647	754-2	V
1057	15 Apr 92	0.8722	957	V
1063	15 Apr 92	1.5831	1139	V
1064	15 Apr 92	1.8847	970	V
1065	15 Apr 92	2.2139	993	V
1066	15 Apr 92	2.4703	1631	V
1067	15 Apr 92	2.7589	1644	V
1068	15 Apr 92	3.0911	3545	V
1069	15 Apr 92	3.4939	3549	V
1070	15 Apr 92	3.7942	3577-1	V
1071	15 Apr 92	4.0628	3577-2	V
1072	15 Apr 92	4.3361	3570	V
1073	15 Apr 92	4.5958	1736	V
1074	15 Apr 92	4.8703	1837	V
1097	16 Apr 92	0.5417	930	V
1098	16 Apr 92	0.7978	1060	V
1099	16 Apr 92	1.1667	979	V
1100	16 Apr 92	1.4514	1020	V
1103	16 Apr 92	1.8692	3490	V
1104	16 Apr 92	2.1153	3505	V
1105	16 Apr 92	2.3469	3528	V
1106	16 Apr 92	2.5967	1709	V
1107	16 Apr 92	3.9458	3562-1	V
1108	16 Apr 92	4.1722	3562-2	V
1109	16 Apr 92	4.4050	3558-1	V
1110	16 Apr 92	4.7130	3558-2	V
1111	16 Apr 92	4.9433	3558-3	V
1112	16 Apr 92	5.2256	3558-4	V
1150	19 Apr 92	0.4019	754-1	V
1151	19 Apr 92	0.6392	754-2	V
1152	19 Apr 92	0.8758	957	V
1153	19 Apr 92	1.1342	970	V
1154	19 Apr 92	1.4047	979	V
1155	19 Apr 92	1.6456	993	V
1156	19 Apr 92	1.8789	1060	V
1157	19 Apr 92	2.1281	1139	V
1158	19 Apr 92	2.3875	1216	V
1159	19 Apr 92	2.6331	1644	V
1161	19 Apr 92	2.8697	1631	V
1162	19 Apr 92	3.1100	3528	V
1163	19 Apr 92	3.3880	3545	V
1164	19 Apr 92	3.6583	3549	V
1165	19 Apr 92	4.0394	3570	V
1165	19 Apr 92	4.5294	1736	V
1189	20 Apr 92	0.1014	930	V
1190	20 Apr 92	0.3281	1020	V
1191	20 Apr 92	0.6152	3490	V
1192	20 Apr 92	0.8594	3505	V
1193	20 Apr 92	1.1503	3559-1	V
1194	20 Apr 92	1.4011	3505	V
1195	20 Apr 92	1.6558	3559-2	V
1196	20 Apr 92	1.9003	3505	V
1197	20 Apr 92	2.1564	3559-3	V
1198	20 Apr 92	2.3989	3559-4	V
1199	20 Apr 92	2.7206	3566-1	V
1200	20 Apr 92	3.0344	3566-2	V
1201	20 Apr 92	3.3469	3571-1	V
1202	20 Apr 92	3.5972	3571-2	V
1203	20 Apr 92	3.8367	3577-1	V
1204	20 Apr 92	4.0831	3577-2	V
1205	20 Apr 92	4.3242	1709	V
1206	20 Apr 92	4.5733	1837	V
1230	21 Apr 92	0.9281	754-1	V
1231	21 Apr 92	1.2750	754-2	V
1232	21 Apr 92	1.5533	957	V
1233	21 Apr 92	1.8069	970	V
1234	21 Apr 92	2.0400	979	V
1235	21 Apr 92	2.2767	993	V

Table 3
continued

Frame No	Date	UT - Middle of exp.	Abell Number	Filter
1236	21 Apr 92	2.5172	1139	V
1237	21 Apr 92	2.7586	1216	V
1238	21 Apr 92	3.0064	3505	V
1239	21 Apr 92	3.2436	3545	V
1240	21 Apr 92	3.4878	3549	V
1241	21 Apr 92	3.7281	3562-1	V
1242	21 Apr 92	4.0458	3562-2	V
1243	21 Apr 92	4.2742	3558-1	V
1244	21 Apr 92	4.5364	3558-2	V
1245	21 Apr 92	4.7580	3558-3	V
1246	21 Apr 92	5.0114	3558-4	V
1247	21 Apr 92	5.9006	1631	V
1248	22 Apr 92	0.4881	930	V
1249	22 Apr 92	0.7428	1020	V
1250	22 Apr 92	0.9911	1060	V
1251	22 Apr 92	2.2844	3559-1	V
1252	22 Apr 92	2.5181	3559-2	V
1253	22 Apr 92	2.7555	3559-3	V
1254	22 Apr 92	3.0428	3559-4	V
1255	22 Apr 92	3.2977	1139	V
1256	22 Apr 92	3.5344	1216	V
1257	22 Apr 92	3.7767	1644	V
1258	22 Apr 92	4.0139	1709	V
1259	22 Apr 92	4.2711	1736	V
1260	22 Apr 92	4.5175	3528	V
1261	22 Apr 92	4.7508	3566-1	V
1262	22 Apr 92	4.9903	3566-2	V
1263	22 Apr 92	5.2328	3571-1	V
1264	22 Apr 92	4.9506	3571-2	V
1265	22 Apr 92	5.6858	3577-1	V
1266	22 Apr 92	5.9200	3577-2	V
1267	22 Apr 92	6.1653	3570	V
1268	22 Apr 92	6.4022	1837	V
1271	7 May 92	0.1808	754-1	V
1272	7 May 92	0.4169	754-2	V
1273	7 May 92	0.6617	1060	V
1274	7 May 92	0.9047	1139	V
1275	7 May 92	1.1436	1216	V
1276	7 May 92	1.3714	1644	V
1277	7 May 92	1.6014	3490	V
1278	7 May 92	1.8281	3505	V
1279	7 May 92	2.0639	3528	V
1280	7 May 92	2.3019	3562-1	V
1281	7 May 92	2.5308	3562-2	V
1282	7 May 92	2.7705	3558-1	V
1283	7 May 92	3.0236	3558-2	V
1284	7 May 92	3.2519	3558-3	V
1285	7 May 92	3.4886	3558-4	V
1286	7 May 92	3.7400	3570	V
1315	7 May 92	23.1956	930	V
1316	7 May 92	23.4228	957	V
1317	7 May 92	23.6514	970	V
1318	7 May 92	23.8817	979	V
1319	8 May 92	0.1664	993	V
1320	8 May 92	0.3939	1020	V
1321	8 May 92	0.6542	1631	V
1322	8 May 92	0.0506	1709	V
1323	8 May 92	1.1689	1736	V
1328	8 May 92	1.6603	3559-1	V
1329	8 May 92	1.8975	3559-2	V
1330	8 May 92	2.1281	3559-3	V
1331	8 May 92	2.3508	3559-4	V
1332	8 May 92	2.5769	3566-1	V
1333	8 May 92	2.8144	3566-2	V
1334	8 May 92	3.0333	3571-1	V
1335	8 May 92	3.2650	3571-2	V
1336	8 May 92	3.4942	3577-1	V
1337	8 May 92	3.7214	3577-2	V
1350	9 May 92	23.4486	1139	V
1351	9 May 92	23.7019	1060	V
1352	9 May 92	23.9717	1216	V
1353	10 May 92	0.2289	3490	V
1354	10 May 92	0.4561	3505	V
1355	10 May 92	0.6952	1631	V
1356	10 May 92	0.9425	1644	V
1361	10 May 92	1.5903	3528	V
1362	10 May 92	1.8572	3562-1	V
1363	10 May 92	2.0964	3562-2	V
1364	10 May 92	2.3464	3558-1	V
1365	10 May 92	2.6014	3558-2	V
1366	10 May 92	2.8383	3558-3	V
1367	10 May 92	3.0831	3558-4	V
1368	10 May 92	3.3774	3545	V
1369	10 May 92	3.6311	3549	V
1370	10 May 92	3.8917	3570	V
1398	11 May 92	0.5703	1709	V
1399	11 May 92	0.8811	1736	V
1400	11 May 92	1.1144	3559-1	V

Table 3
continued

Frame No	Date	UT - Middle of exp.	Abell Number	Filter
1401	11 May 92	1.3692	3559-2	V
1402	11 May 92	1.6078	3559-3	V
1403	11 May 92	1.8450	3559-4	V
1404	11 May 92	2.0836	3566-1	V
1405	11 May 92	2.9797	3566-2	V
1406	11 May 92	3.2147	3571-1	V
1407	11 May 92	3.4906	3571-2	V
1408	11 May 92	3.8011	3577-1	V
1409	11 May 92	4.0378	3577-2	V
1410	11 May 92	4.2839	1837	V
1411	11 May 92	4.6106	2052	V
1412	11 May 92	4.9586	2063	V
1427	12 May 92	2.8175	3562-1	V
1428	12 May 92	3.0422	3562-2	V
1429	12 May 92	3.2836	3545	V
1430	12 May 92	3.5306	3549	V
1431	12 May 92	3.7783	3570	V
1432	12 May 92	4.0272	3558-1	V
1433	12 May 92	4.2717	3558-2	V
1434	12 May 92	4.5125	3558-3	V
1435	12 May 92	4.7597	3558-4	V
1455	12 May 92	23.8864	754-1	V
1456	13 May 92	0.1272	754-2	V
1457	13 May 92	0.3858	930	V
1458	13 May 92	0.6344	957	V
1459	13 May 92	0.9092	970	V
1460	13 May 92	1.1683	979	V
1461	13 May 92	1.4055	993	V
1462	13 May 92	1.7756	1060	V
1509	15 May 92	23.6528	754-1	V
1510	16 May 92	0.0814	930	V
1511	16 May 92	0.3406	754-2	V
1512	16 May 92	0.5894	957	V
1513	16 May 92	0.8847	970	V
1514	16 May 92	1.1369	979	V
1523	16 May 92	23.8747	1020	V
1524	17 May 92	0.1292	1060	V
1525	17 May 92	0.3733	1139	V
1528	17 May 92	0.7667	1216	V
1529	17 May 92	1.0275	3490	V
1530	17 May 92	1.2703	1060	V
1531	17 May 92	1.5208	3505	V
1532	17 May 92	1.7767	3528	V
1533	17 May 92	2.0355	3562-1	V
1534	17 May 92	2.2644	3562-2	V
1535	17 May 92	2.5250	3545	V
1536	17 May 92	2.7614	3549	V
1542	29 May 92	23.8764	754-1	V
1543	30 May 92	0.1372	754-2	V
1544	30 May 92	0.3772	1020	V
1545	30 May 92	0.6253	1060	V
1546	30 May 92	0.8733	1139	V
1547	30 May 92	1.1222	3490	V
1548	30 May 92	1.3622	3505	V
1549	30 May 92	1.6214	3528	V
1550	30 May 92	1.8758	3570	V
1584	30 May 92	23.5494	930	V
1585	30 May 92	23.7817	957	V
1586	31 May 92	0.0328	970	V
1587	31 May 92	0.2892	979	V
1588	31 May 92	0.5481	993	V
1589	31 May 92	0.7939	3558-1	V
1590	31 May 92	1.0278	3558-2	V
1591	31 May 92	1.2753	3558-3	V
1592	31 May 92	1.5183	3558-4	V
1593	31 May 92	1.7792	3562-1	V
1594	31 May 92	2.0336	3562-2	V
1598	31 May 92	3.2378	3559-2	V
1599	31 May 92	3.4661	3559-3	V
1600	31 May 92	3.7039	3559-4	V
1601	31 May 92	3.9531	3559-4	V
1620	1 Jun 92	0.0839	1216	V
1621	1 Jun 92	0.3181	1631	V
1622	1 Jun 92	0.5533	1644	V
1623	1 Jun 92	0.7878	1709	V
1624	1 Jun 92	1.0281	1736	V
1625	1 Jun 92	1.2772	3566-1	V
1626	1 Jun 92	1.5242	3566-2	V
1627	1 Jun 92	1.7642	2052	V
1658	2 Jun 92	2.1383	3545	V
1659	2 Jun 92	2.3761	3549	V
1660	2 Jun 92	2.6786	3571-1	V
1672	2 Jun 92	23.7250	754-1	V
1673	2 Jun 92	23.9614	754-2	V
1674	3 Jun 92	0.1964	3571-1	V
1675	3 Jun 92	0.4492	3571-2	V
1676	3 Jun 92	0.6925	3577-1	V
1677	3 Jun 92	0.9239	3577-2	V

Table 3
continued

Frame No	Date	UT - Middle of exp.	Abell Number	Filter
1678	3 Jun 92	1.1658	3528	V
1679	3 Jun 92	1.4222	1837	V
1682	3 Jun 92	1.8314	2063	V
1683	3 Jun 92	2.2789	3558-1	V
1684	3 Jun 92	2.5089	3558-2	V
1685	3 Jun 92	2.7397	3558-3	V
1686	3 Jun 92	2.9879	3558-4	V
1687	3 Jun 92	3.3028	3570	V
1690	3 Jun 92	3.7617	2052	V
1711	3 Jun 92	23.9261	957	V
1712	4 Jun 92	0.1554	957	V
1713	4 Jun 92	0.4044	970	V
1714	4 Jun 92	0.6533	979	V
1715	4 Jun 92	0.9128	993	V
1716	4 Jun 92	1.1442	1020	V
1717	4 Jun 92	1.3744	1060	V
1718	4 Jun 92	1.6117	1139	V
1721	4 Jun 92	2.6161	3562-1	V
1722	4 Jun 92	2.8528	3562-2	V
1723	4 Jun 92	3.0936	3559-1	V
1724	4 Jun 92	3.4128	3559-2	V
1750	30 Jun 92	2.2919	3570	V
1751	30 Jun 92	2.5397	3571-1	V
1752	30 Jun 92	2.8096	3571-2	V
1753	30 Jun 92	3.0739	3577-1	V
1754	30 Jun 92	3.3439	3577-2	V
1755	30 Jun 92	3.6642	1837	V
1756	30 Jun 92	3.9881	2052	V
1757	30 Jun 92	4.2994	2063	V
1758	30 Jun 92	4.8742	3651	V
1759	30 Jun 92	5.2353	3667	V
1762	1 Jul 92	8.7831	3677	V
1763	1 Jul 92	9.1819	3703	V
1764	1 Jul 92	9.4608	3716	V
1765	1 Jul 92	9.7167	3733	V
1766	1 Jul 92	9.9936	3806	V
1767	1 Jul 92	10.3667	3822	V
1768	1 Jul 92	10.7753	2382	V
1769	1 Jul 92	23.1133	3505	V
1770	1 Jul 92	23.3536	3558-1	V
1800	2 Jul 92	8.8236	3806-2	V
1801	2 Jul 92	9.0527	3806-3	V
1802	2 Jul 92	9.4119	3825	V
1803	2 Jul 92	9.7017	3826	V
1856	5 Jul 92	1.3194	3562-2	V
1857	5 Jul 92	1.5481	3566-1	V
1858	5 Jul 92	1.7350	3566-2	V
1875	5 Jul 92	8.7978	4038-2	V
1876	5 Jul 92	9.1033	4038-1	V
1877	5 Jul 92	9.3622	4038-1	V
1878	5 Jul 92	9.8450	4059	V
1879	5 Jul 92	10.2969	2670	V
1880	5 Jul 92	10.5989	2717	V
1881	5 Jul 92	23.2181	3545	V
1882	5 Jul 92	23.4397	3549	V
1883	5 Jul 92	23.8747	1709	V
1884	6 Jul 92	0.1044	1736	V
1885	6 Jul 92	0.3108	3559-1	V
1886	6 Jul 92	0.5289	1644	V
1926	6 Jul 92	9.6633	2933	V
1928	6 Jul 92	10.3397	2995	V
1944	7 Jul 92	8.4847	2399	V
1945	7 Jul 92	9.1083	2657	V
1949	7 Jul 92	22.8933	930	V
1950	8 Jul 92	3.4481	970	V
1951	7 Jul 92	23.7928	1060	V
1984	9 Jul 92	7.4783	3651	J
1985	9 Jul 92	7.6911	3667	J
1986	9 Jul 92	8.4864	3677	J
1987	9 Jul 92	8.6964	3733	J
1988	9 Jul 92	8.9494	2382	J
1989	9 Jul 92	9.2047	3806	J
1990	9 Jul 92	9.4561	3822	J
1991	9 Jul 92	9.6777	3806-2	J
1992	9 Jul 92	23.1469	3528	J
1993	9 Jul 92	23.4389	1631	J
1994	9 Jul 92	23.7553	1644	J
1995	10 Jul 92	0.1319	3545	J
1996	10 Jul 92	0.3669	3549	J
1997	10 Jul 92	0.6194	1709	J
1998	10 Jul 92	0.8719	1736	J
1999	10 Jul 92	1.1161	3558-1	J
2000	10 Jul 92	1.3603	3558-2	J
2001	10 Jul 92	1.5955	3558-3	J
2002	10 Jul 92	1.8417	3558-4	J
2032	10 Jul 92	6.9836	3716	J
2033	10 Jul 92	7.2492	3806-3	J
2034	10 Jul 92	7.6056	2399	J

Table 3
continued

Frame No	Date	UT - Middle of exp.	Abell Number	Filter
2035	10 Jul 92	7.8998	4038-1	J
2036	10 Jul 92	8.1292	4038-2	J
2037	10 Jul 92	8.3725	4059	J
2038	10 Jul 92	8.6228	2670	J
2039	10 Jul 92	8.8744	2657	J
2040	10 Jul 92	9.1430	3825	J
2041	10 Jul 92	9.4392	3826	J
2044	10 Jul 92	10.2764	2717	J
2046	10 Jul 92	23.7078	979	V
2047	10 Jul 92	23.9581	1060	V
2048	11 Jul 92	0.1942	1216	V
2049	11 Jul 92	0.5644	3490	V
2050	11 Jul 92	0.8350	3490	J
2051	11 Jul 92	1.0972	3528	J
2052	11 Jul 92	1.4866	1631	V
2053	11 Jul 92	1.8444	3559-1	J
2054	11 Jul 92	2.0919	3559-2	J
2055	11 Jul 92	2.3558	3559-2	V
2056	11 Jul 92	2.5994	3559-3	J
2057	11 Jul 92	2.8417	3559-4	J
2059	11 Jul 92	3.5447	3651	V
2060	11 Jul 92	3.8039	3667	V
2061	11 Jul 92	4.0969	3677	V
2062	11 Jul 92	4.3664	3703	V
2063	11 Jul 92	4.6906	3703	J
2064	11 Jul 92	4.9492	3716	V
2065	11 Jul 92	5.1925	3733	V
2069	11 Jul 92	6.7169	3806	V
2070	11 Jul 92	6.9856	3822	V
2071	11 Jul 92	7.2319	2382	V
2072	11 Jul 92	7.4728	3806-2	V
2073	11 Jul 92	7.7297	3806-3	V
2074	11 Jul 92	7.9761	3825	V
2075	11 Jul 92	8.2369	2399	V
2076	11 Jul 92	8.4747	3826	V
2077	11 Jul 92	8.9014	4038-1	V
2078	11 Jul 92	9.1547	4038-2	V
2079	11 Jul 92	9.4050	4059	V
2080	11 Jul 92	9.6886	2657	V
2084	15 Jul 92	23.5675	3562-1	J
2085	15 Jul 92	23.7564	3562-2	J
2086	16 Jul 92	0.0092	3566-1	J
2087	16 Jul 92	0.2244	3566-2	J
2088	16 Jul 92	0.4497	3570	J
2103	16 Jul 92	6.5314	3667	J
2104	16 Jul 92	6.7989	3667	J
2105	16 Jul 92	7.0414	3667	V
2120	18 Jul 92	7.6742	3651	V
2121	18 Jul 92	7.9219	3667	V
2122	18 Jul 92	8.1641	3703	V
2123	18 Jul 92	8.4105	3716	V
2124	18 Jul 92	8.6786	3806	V
2125	18 Jul 92	8.9147	3822	V
2126	18 Jul 92	9.2128	3825	V
2127	18 Jul 92	9.4558	3826	V
2128	18 Jul 92	9.6853	4059	V
2129	18 Jul 92	9.9331	2717	V
2169	19 Jul 92	7.4178	3677	V
2170	19 Jul 92	7.6558	3733	V
2171	19 Jul 92	7.9092	3806-2	V
2172	19 Jul 92	8.1533	3806-3	V
2173	19 Jul 92	8.4100	4038-1	V
2174	19 Jul 92	8.6528	4038-2	V
2175	19 Jul 92	8.9075	2657	V
2176	19 Jul 92	9.1497	2670	V
2177	19 Jul 92	9.4683	2933	V
2178	19 Jul 92	9.7014	2995	V
2182	19 Jul 92	23.1864	3571-1	J
2183	19 Jul 92	23.4494	3571-2	J
2184	19 Jul 92	23.6583	3577-1	J
2185	19 Jul 92	23.9042	3577-2	J
2223	20 Jul 92	8.4733	2382	V
2224	20 Jul 92	8.7225	2399	V
2225	20 Jul 92	8.9914	4059	V
2226	20 Jul 92	9.2694	2933	J
2227	20 Jul 92	9.5242	2995	J
2228	20 Jul 92	9.7558	2995	V
2233	20 Jul 92	23.2731	1644	V
2234	20 Jul 92	23.5406	1709	V
2235	20 Jul 92	23.8053	3549	V
2236	21 Jul 92	0.2047	3545	V
2267	21 Jul 92	8.8194	3822	V
2268	21 Jul 92	9.0597	3825	V
2269	21 Jul 92	9.3205	3826	V
2271	21 Jul 92	10.0564	2717	V
2274	21 Jul 92	23.0608	2052	V
2275	21 Jul 92	23.2992	2063	V

Table 3
continued

Frame No	Date	UT - Middle of exp.	Abell Number	Filter
2307	22 Jul 92	8.1408	3703	V
2308	22 Jul 92	8.4244	3716	V
2309	22 Jul 92	8.7353	3806	V
2310	22 Jul 92	9.0414	2657	V
2311	22 Jul 92	9.3125	2670	V
2312	22 Jul 92	9.5528	2933	V
2313	22 Jul 92	9.7878	2995	V
2317	22 Jul 92	23.2161	3571-1	V
2318	22 Jul 92	23.4831	3571-2	V
2331	23 Jul 92	23.1080	1736	V
2332	23 Jul 92	23.4503	3558-1	V
2333	23 Jul 92	23.6703	3558-2	V
2334	23 Jul 92	23.8950	3558-3	V
2355	24 Jul 92	6.5728	3733	V
2356	24 Jul 92	6.8533	2382	V
2357	24 Jul 92	7.1311	2399	V
2358	24 Jul 92	7.4731	4038-1	V
2359	24 Jul 92	7.7256	4038-2	V
2360	24 Jul 92	8.0228	4059	V
2364	24 Jul 92	9.4808	2717	V
2365	25 Jul 92	22.9669	3559-3	V
2366	25 Jul 92	23.2000	3559-4	V
2367	25 Jul 92	23.4361	3562-1	V
2368	25 Jul 92	23.6631	3562-2	V
2392	26 Jul 92	6.9319	3651	V
2393	26 Jul 92	7.2039	3822	V
2394	26 Jul 92	7.4572	3806-2	V
2395	26 Jul 92	7.8139	3806-3	V
2396	26 Jul 92	8.0403	3825	V
2397	26 Jul 92	8.3250	3826	V
2400	26 Jul 92	9.4600	2657	V
2401	26 Jul 92	9.6847	2670	V
2402	26 Jul 92	9.9203	2933	V
2403	26 Jul 92	10.1556	2995	V
2405	26 Jul 92	23.3022	3558-4	V
2406	26 Jul 92	23.5711	3559-1	V
2407	26 Jul 92	23.8119	3566-1	V
2432	27 Jul 92	6.4844	3677	J
2433	27 Jul 92	6.7425	3703	J
2434	27 Jul 92	7.0186	3716	J
2435	27 Jul 92	7.2931	3733	J
2436	27 Jul 92	7.6033	3806	J
2438	27 Jul 92	7.9361	3806-2	J
2439	27 Jul 92	8.2611	3806-3	J
2442	27 Jul 92	9.4319	4038-2	J
2443	27 Jul 92	9.6786	4038-1	J
2444	27 Jul 92	9.9347	4059	J
2445	27 Jul 92	10.2305	2717	J
2446	28 Jul 92	23.1364	3566-2	V
2482	30 Jul 92	6.5239	3667	V
2483	30 Jul 92	6.7728	3677	V
2484	30 Jul 92	7.0256	3716	V
2485	30 Jul 92	7.2767	3733	V
2486	30 Jul 92	7.6264	3806	V
2487	30 Jul 92	8.1361	3822	V
2488	30 Jul 92	8.3794	2382	V
2489	30 Jul 92	8.6461	2399	V
2490	30 Jul 92	8.8983	4059	V
2491	30 Jul 92	9.1453	2670	V
2494	30 Jul 92	10.1778	2933	V
2495	30 Jul 92	10.3833	4038-2	V
2519	6 Aug 92	6.1411	3677	V
2520	6 Aug 92	6.4011	2382	V
2521	6 Aug 92	6.6614	2399	V
2522	6 Aug 92	6.9636	4038-2	V
2523	6 Aug 92	7.2378	4059	V
2524	6 Aug 92	7.4753	2657	V
2525	6 Aug 92	7.7319	2670	V
2528	6 Aug 92	8.6892	2717	V
2529	6 Aug 92	9.1592	2933	V
2530	6 Aug 92	9.3939	2995	V
2640	9 Aug 92	5.6933	3677	V
2641	9 Aug 92	5.9436	3667	V
2642	9 Aug 92	6.2050	3703	V
2643	9 Aug 92	6.4628	3716	V
2644	9 Aug 92	6.6950	3733	V
2645	9 Aug 92	6.9342	3806	V
2646	9 Aug 92	7.1719	3822	V
2647	9 Aug 92	7.4111	2382	V
2648	9 Aug 92	7.6567	4038-2	V
2649	9 Aug 92	7.8878	4059	V
2650	9 Aug 92	8.1009	2670	V
2651	9 Aug 92	23.1922	3559-3	V
2652	9 Aug 92	23.4256	3559-4	V
2653	9 Aug 92	23.6636	3562-1	V
2654	9 Aug 92	23.8972	3562-2	V
2692	10 Aug 92	3.5236	3651	V

Most of the observations were obtained in an infrared filter closely matching the Gunn i filter. A few frames were also acquired in Johnson V filter for all fields. The exposure times varied depending on the seeing conditions; typical times were 10 minutes in I and 12 minutes in V . Because of the lengthy readout and preparation times for the CCD, the effective time between exposures was at least 3 minutes longer than the exposure times.

During periods of poor seeing (*i.e.* greater than 1.7 arcsec) or when the Bulge was simply too low to be observed, we obtained images of a number of clusters of galaxies to search for supernovae. Table 2 lists the clusters we observed, along with their coordinates and the number of frames we collected for each. Most of the observations were obtained using the V filter, and the exposure times were generally 10 minutes. For several clusters, I -band images were also secured. Table 3 gives a full log of the cluster observations.

On six photometric nights, we observed a number of Landolt standard fields (Landolt 1992) to calibrate our photometry. The mean coefficients derived from these observations to transform our photometry to the standard Johnson V and Cousins I band are listed in Table 4. The instrumental magnitudes were shifted so that for a typical Bulge object ($V - I \approx 1.2$) they are equal to the system magnitude. Though the internal consistency of the absolute magnitudes derived on different nights was within 0.02 mag, we cannot rule out some systematic errors up to 0.05 mag for the Bulge object magnitudes. Because of extreme crowding in the Bulge fields, reliable determination of the aperture photometry of the Bulge stars was particularly difficult. The aperture correction for each CCD field was typically derived from the median of the measurements of about 1000 of the brightest stars on the frame.

Table 4

Transformation to the Standard V/I System.

$$\begin{aligned}
 V &= v + 0.032 \times (V - I) - 0.038 \\
 &\quad \pm 0.005 \qquad \qquad \qquad \pm 0.015 \\
 I &= i - 0.018 \times (V - I) + 0.017 \\
 &\quad \pm 0.006 \qquad \qquad \qquad \pm 0.021 \\
 V - I &= 1.047 \times (v - i) - 0.061 \\
 &\quad \pm 0.008 \qquad \qquad \qquad \pm 0.019
 \end{aligned}$$

Of the 65 nights allocated to this project, 49 were useful or partially useful, or a total of 75%. This is better than typical of the fall/winter at LCO. However, it should be stressed that due to El Niño phenomenon in 1992 and Pinatubo volcano eruption only small fraction (about 20%) of the useful nights were truly photometric which is much worse than typical at LCO.

3. Reductions

Due to the huge amount of data coming from the telescope, a dedicated hardware/software system was developed to handle the data flow. During each clear night about 40-50 frames and several calibration frames were collected. This implies a nightly data rate of about 0.5 – 0.6 Gbytes. The data system was designed to identify automatically all new data frames coming from the telescope, calculate the seeing and mean sky levels of the CCD images and perform all necessary reductions "on-the-fly", including profile photometry. Because of hardware limitations, some small parts of this process were never implemented in a fully automatic manner during the 1992 observations. Nevertheless, the data system significantly reduced the burden on the observers during the observations.

3.1. Preliminary Reductions

The first stage of the reduction process occurred on a standard LCO Sun 386i data acquisition computer. The local data acquisition program was significantly modified to synchronize it with the various external CCD processing programs. These included two "daemons" with the following tasks: the first Unix daemon identified a newly-acquired frame and asked the observer to confirm the type of observed object (*i.e.* Bulge, cluster of galaxies, or standards) and whether further processing was desired for the frame. This was the last opportunity for the observer to interfere interactively with a just-acquired frame. Upon approval for further reduction, the first daemon notified an IRAF² daemon which performed two operations: a) the mean FWHM of isolated bright stars on each frame was determined and written to the image header, b) the frames were then converted from Sun 386i to Sun Sparc format (byte swapping and some minor operations), and automatically transferred to another computer over the Ethernet network at LCO.

The reduction computer used for the project was a Sun Microsystems SparcStation 2, with 64 MBytes memory, 3.7 GBytes disks and an EXB-8500 Exabyte tape drive. This computer was dedicated for the reduction of the microlensing CCD data. Some additional reductions were performed on a local SparcStation 2 located permanently at LCO.

On the SparcStation, another daemon waited for frames arriving from the Sun 386i computer. Frames of all types were automatically de-biased and flat-fielded using the previously prepared calibration frames and IRAF "ccdred" routines. The sky level was derived as follows. For standard and cluster frames the sky was assumed as a median of pixel statistic in five selected subfields of the frame. For extremely crowded Bulge fields the sky level was very hard to define. We finally adopted the sky for these fields to be equal to the value corresponding to the lowest

² IRAF is distributed by National Optical Astronomy Observatories, which is operated by the Association of Universities for Research in Astronomy, Inc., under cooperative agreement with the National Science Foundation.

1% of the pixel value distribution. It turned out that even at this low level, we generally overestimated the sky level in the Bulge frames. Fortunately, only a crude estimate of the sky level was necessary for further reductions. The SparcStation daemon then wrote sky value into the frame header and subsequently converted the frame to FITS format with scaling appropriate for the frame type (*i.e.* no scaling for Bulge frames).

3.2. Photometry

The final reductions at the telescope were performed for the Bulge frames only. The DoPHOT photometry program (Mateo and Schechter 1989) was used to derive profile-fitting photometry of the stars in these frames. A number of changes, bug fixes and specialized improvements were incorporated into the standard 2.0 version of this software. The most important changes included:

- The introduction of a new sky algorithm based on a median smoothing of the star-subtracted picture;
- The use of a new binary output format which significantly speeded up I/O operations and saved disk space;
- Dynamic allocation of arrays, making the size of the program much smaller;
- Quadratic coordinate transformations in the fixed-position mode of the program (see below).

The DoPHOT reduction of the frames was intended to run as the final step of the automatic data-processing software system for the observing run. In practice, it turned out that the data flow was too large to be handled by the two computers available; thus, because of this and disk space limitations, we decided to run the final DoPHOT reductions by hand, temporarily storing unreduced frames on Exabyte tapes. During the gaps between the subruns, the reductions of the remaining frames from the previous subrun were completed.

We used the DoPHOT program in the fixed-position mode. In this mode the program fits only five independent parameters (local sky, central intensity and three image shape parameters) to the highest S/N stellar images, keeping the x and y position fixed to a predetermined constant value. The stellar positions were provided from a list of the output photometry taken from the reduction of a "template" image of the same field. In practice, the template frame was chosen to be one obtained in very good seeing conditions, and reduced using the regular mode of DoPHOT in which the positions are not fixed. The fixed-position mode has two very important advantages: it significantly speeds up the reductions, and provides more repeatable results – compared to standard DoPHOT – for frames taken in different seeing conditions even in dense Bulge fields. By using an input template file, DoPHOT "knows" that images obtained in poorer seeing conditions are composed of two stars, rather than trying to fit the profile as a single star. Because the sizes of various fitting and aperture photometry boxes used by DoPHOT scale directly with the typical size of the stellar images, the reduction rate is a strong function of

the seeing. For frames taken at very good seeing conditions, our enhanced version of DoPHOT reached 10^5 stars/hour/CPU, while for frames with poor seeing, the rate dropped to about 3×10^4 stars/hour/CPU.

Our first experiments with DoPHOT on Bulge frames showed that it is not possible to obtain reliable photometry reducing the whole frame assuming a constant point spread function (PSF). The PSF changes significantly across the Ford chip due to its surface non-uniformities, and to a much lesser extent, telescope aberrations. This required us to develop a new method of reducing these data utilizing the existing version of DoPHOT available during the observing run. This method is based on dividing the frame into small "subframes" in which the PSF is much more likely to be constant. The method works best in dense fields where the number of stars is sufficiently high to assure a precise photometric tie between adjacent subframes (changing the PSF in each subframe has the effect of systematically offsetting the photometry from each region; the overlap regions were used to determine these offsets). The Bulge fields are ideal for this because of the very large number of stars in the overlap regions. After some experimentation, we found that a 7×7 grid of subframes was optimum; this corresponds to 300×300 pixel subframes. Our tests showed that on such a small subframe the PSF was indeed stable and photometry was very reliable. The number of stars on a subframe was typically 3000 – 8000. Fig. 2 shows a diagram frame *minus* template magnitude of the same object vs.

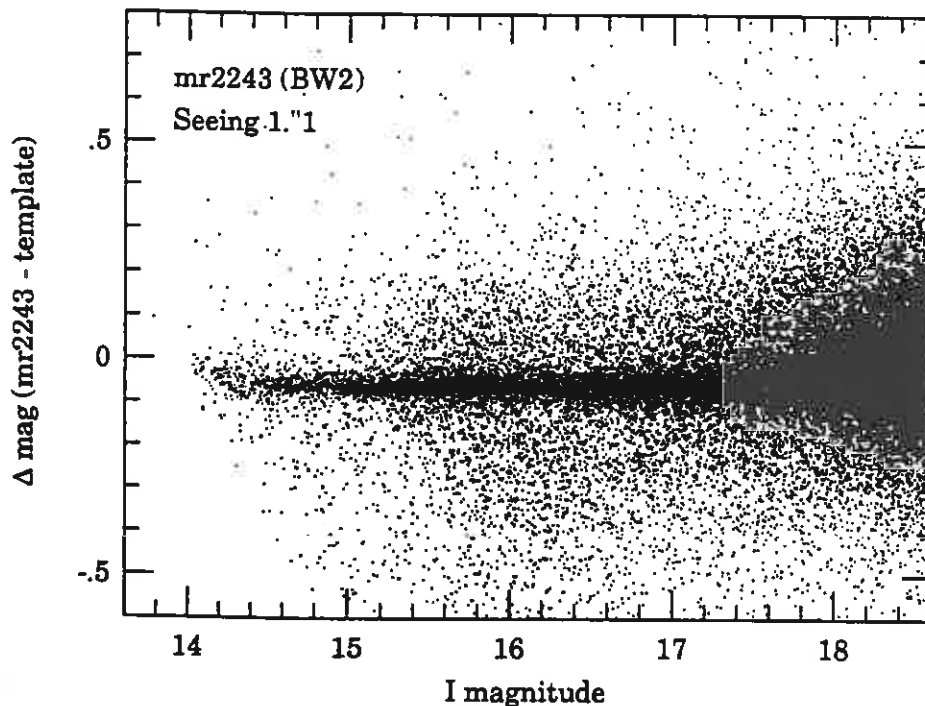


Fig. 2. The difference of magnitudes "frame *minus* template" obtained by reducing the whole frame with constant PSF.

template magnitude for photometry obtained by running the DoPHOT on the whole frame with constant PSF. This diagram can be compared with Fig. 3 showing analogous diagram for photometry derived using the frame-dividing algorithm. The improvement of the quality of the photometry is dramatic.

The reduction method described above imply that two distinct procedures had to be applied to the data for each field we observed. First, the photometry and positions of objects from the template frame had to be derived. Second, the remaining frames had to be reduced using the results from the template for that field. To do this in a consistent manner, each template was divided into a grid of 7×7 subframes. Each subframe overlapped with the adjacent ones by 100 pixels. Two reduction passes were then performed on each subframe of the template frame. In the first pass DoPHOT was run in its regular mode without fixed positioning. In the second pass, the results from the first pass were used as the template, and DoPHOT was run in its fixed-position mode. In this manner, we picked up all stars left in the regular mode pass in order to create the most complete template list possible. If cosmic rays or noise spikes were included, subsequent passes with DoPHOT would tend to fail to find real stellar images at the corresponding positions; such cases would be easily distinguished from real stars. Using the brighter stars in the overlapping strips between subframes, appropriate magnitude corrections were calculated. Typically about 100 stars were used to calculate each of these corrections. Apart from the boundary subframes, all other subframes could be tied together in a number of different ways using different combinations of other subframes. This served as an independent test of the reliability of the method. In no case did the difference exceed 0.005 mag, indicating that the final photometry was indeed on a common photometric system. Finally, the derived corrections were added to results of photometry and each subframe was trimmed to overlap with the adjacent one by 30 pixels only. This was necessary to minimize the number of stars lying close to the boundary and having photometry on both subframes. The minimum overlap was necessary to ensure good photometry of all stars in boundary regions. The trimmed subframes served as "sub-templates" for the corresponding subframes of the remaining frames of the field.

The reductions of the non-template frames of a given field consisted of three steps. First, the coordinate shift between the frame and its template was calculated using a similar-triangle method (Groth 1986). The frame was then divided into subframes with boundaries coincident with the subframe boundaries of the template frame (to within ± 1 pixel). This method allowed us to minimize the area for which template was not available for frames that were not perfectly aligned with their templates. If any resulting subframe was smaller than 100 pixels in any dimension, it was removed and the photometry for that subframe was not performed. The typical shift to achieve template alignment was a few pixels; however, on occasion much larger shifts occurred due to gross pointing errors. In the second step, PSF photometry was performed on the frame using the fixed-position mode in DoPHOT

with the appropriate sub-template. In the third step, the photometry of the subframe obtained in step two was tied to the template photometric system. This was done by calculating the mean magnitude differences of stars in common to the two frames and adding the appropriate corrections to the photometry of the subframe. Finally, the results of all the subframes were grouped into two files. The first contained the photometry of all objects which were also detected on the sub-templates, while the second contained the photometry of any new objects detected on the subframe but not found in the template. Any results from areas of the frame that did not overlap with the template were omitted. The photometry of the stars in these regions could have been performed using the regular mode of DoPHOT, but the results would have been on a somewhat different photometric system and would have had a slightly different distribution of photometric errors. The omitted area rarely exceeded 5% of the total image area; the loss of these few stars is clearly not significant.

All the reduction procedures described above were performed automatically. The only required input information was the frame number. Frame division, preparation of DoPHOT input file (containing the names of the input/output/template files, the sizes of various fitting boxes which were calculated relative to the seeing, and threshold information calculated relative to the estimated sky for the frame and the CCD noise properties), running DoPHOT on each subframe, *etc.* was done fully automatically. The output of this process were files containing the photometry of all identified stars on the input frame. In order to avoid spurious results due to chip defects, a map of bad and hot pixels was determined. It was used by DoPHOT as an input file to allow the program to obliterate the defects and ignore the offending pixels during the reduction.

It was apparent to us from the outset, that the template frames should be obtained as soon as possible in the observing run because their existence would be necessary for all subsequent photometry. Fortunately, some of the best seeing of the entire run occurred during the first two subruns, and we obtained the templates for almost every field early in the observational season. The final templates were selected from well-guided frames, obtained on dark nights with seeing in the range 0.95 – 1.15 arcsec. Thanks to this bit of good luck, about 90% of all the Bulge frames were reduced by the end of the whole run.

3.3. *The Final Database*

The final step of the reduction procedure was to group together the results for all frames of each field. Because the number of stars detected in some of the fields exceeded 2.5×10^5 and such fields were observed approximately 50 times, very efficient tools for data manipulation had to be written. A database was constructed for each field and filter. Each database consists of a few files containing all important data from the photometry. These include the following:

1. A catalog of the frames containing the times of observation (UT and heliocentric Julian Date), exposure times, number of objects found, and the grade of the photometry (see Section 4).
2. An index of frames giving in chronological order the position of the frame within the database. This allows adding the frames to the database in any sequence, not necessarily chronological.
3. A catalog of "template objects" corresponding to objects found on every frame that has a counterpart in the template file. The catalog contains coordinates (in pixels) of objects in the coordinate system of the template image. For all objects found in overlapping regions of the subframes, a pointer to next "same" object is given, as well as the total number of the occurrences. There is also a flag set for objects which are outside the overlapping regions but still are closer than 0.25 pixel. The flag is also set for objects which are located within 8 pixels from the edge of the subframe. The catalog contains three additional data fields to allow rapid identification of possible variability: the sum of magnitudes of "good" photometry points, the sum of their squares and the number of "good" points. These values are updated every time a new frame results are added. A "good" point represents a measurement that received a DoPHOT image type of 1, 3 or 7 (these correspond to bright stars, individual components of double stars, and faint objects classified as stars) and which is not flagged for illegal multiplicity, location near the edge of a subframe, *etc.* These three fields will be useful during future observing runs when we expect the results will be added to the database almost on-line.
4. A photometry data file for "template objects" containing the measured magnitude, formal error, and DoPHOT object type for each object. The type field also contains a "packed" (in order to save disk space) magnitude flag which, if set, indicates that the magnitude of any "multiple" object (*i.e.* one measured two to four times in the subframe overlap regions) differs from its mean magnitude by more than 0.25 mag.
5. A catalog of "new objects" not found in template list. This catalog contains the coordinates and sums of magnitude values as in the template catalog file. In addition, the position of the first occurrence in the photometry data file (item 6) is given, allowing fast access to the data for any object. The catalog also contains the number of occurrences of the new object within the database. An object from the photometry result file is considered to be a later occurrence of a previously found new object if the image separation is less than 0.25 pixel.
6. A photometry file for "new objects" containing in addition to the magnitude, its formal error and the object type, the position of the next occurrence of the same object in the photometry file. The position of the first entry is kept in the catalog file described in item 5 above. These positions are required because this photometry file has a "free" format as opposed to the template objects photometry file which, by definition, contains the same number of objects in every frame. The number of new objects differs from frame to frame and is expected to grow as more frames

are obtained; thus this photometry file must be self-indexed. For the same reason the number of the frame from which the measurement is taken must also be kept in this file.

To allow fast and easy access to the database a small library of user-callable subroutines have been written (available in C and Fortran). These functions can be used to open one or more databases (considered as sets of described above files containing the data for a given Bulge field and filter), obtain the number of frames and objects, as well as the catalog information and photometric data for any individual object.

All the collected images will be available for astronomical community from the NASA NSS Data Center from January 1, 1993. We plan to store the calibrated FITS format images of both the Galactic Bulge and clusters of galaxies in this database. After one year, the entire database including the reduced photometry will also be available at the NSSDC for all of the observed fields, as well as the support software.

4. Results

A total of 675 *I* and 152 *V* CCD frames of the 14 Galactic Bulge fields were collected over the course of the entire run. Except for 24 *I* and 13 *V* short exposure frames, all remaining images were processed and reduced using the methods described in Section 3. Not surprisingly, it turned out that in the dense Bulge fields the quality of the photometry is critically dependent on the seeing. Fig. 3 shows the difference in magnitudes for stars measured in an object frame and its corresponding template frame in the sense frame *minus* template *vs.* template magnitude for two frames of the same field taken at different seeing conditions: 1.1 and 1.9 arcsec. It is apparent that the photometry in the latter case is significantly worse than the results from the good-seeing frame. After comparisons of a number of frames in different seeing conditions, we decided early in the run to limit the Bulge observations to periods when the seeing was better than than 1.7 arcsec. For the densest frames an even stronger constraint (1.5 arcsec) was imposed.

Although the seeing was the most important factor of the quality of photometry, we found it was possible to compensate for it somewhat (within the constraints described above) by increasing up to 15 minutes the exposure times during the periods of poorer seeing. Other factors also influenced the quality of the photometry. The most important included errors in telescope tracking and poor focusing; these effects resulted in somewhat elongated images, and – in the case of poor focus – PSF variations over the chip. Some of frames were taken through the clouds, effectively shortening the exposure times by an uncertain amount. Thin cirrus generally did not spoil the photometry for the majority of the stars in the program fields, however, partly because the seeing would often noticeably improve during periods of thin, high-level cloud cover.

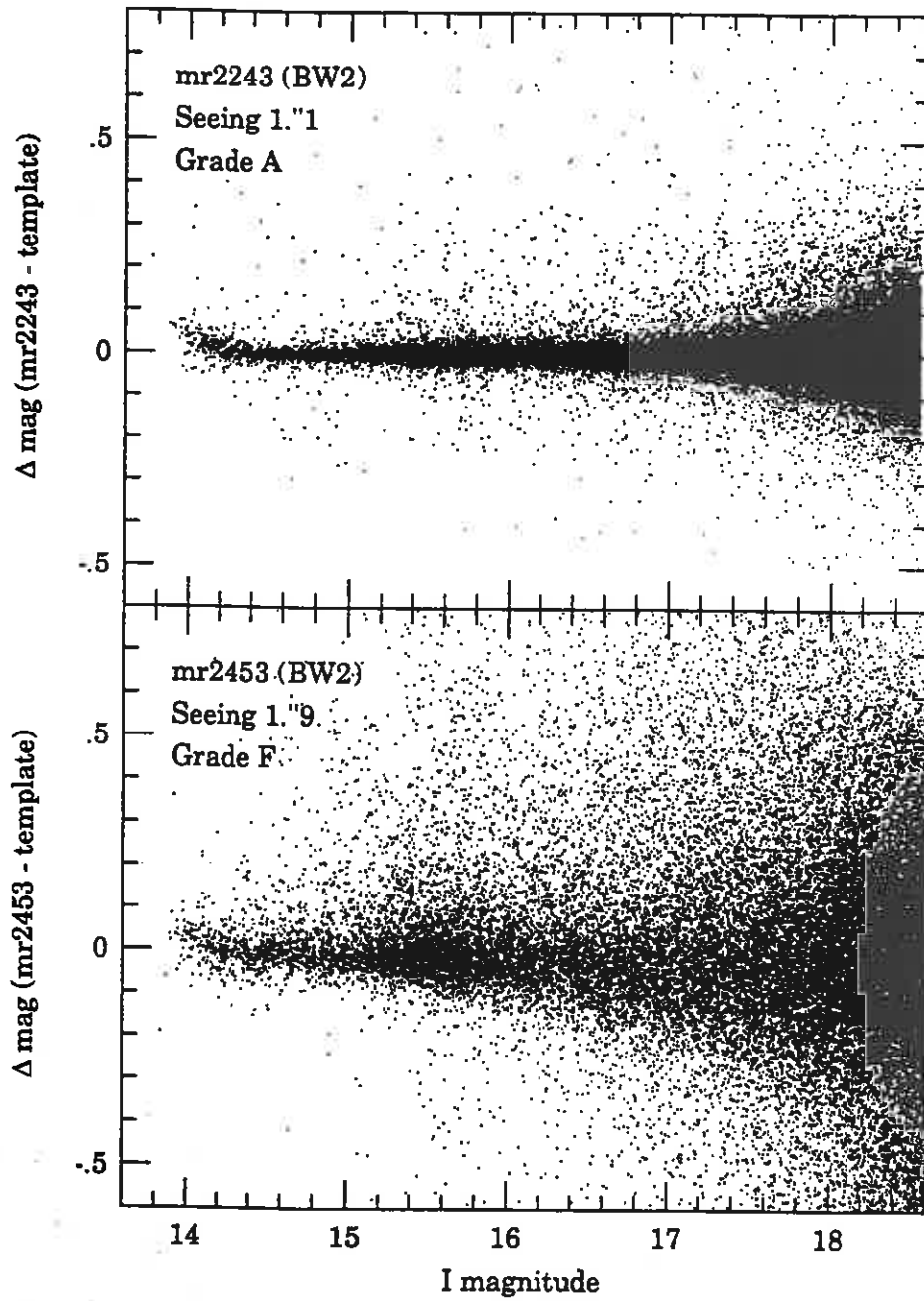


Fig. 3. The difference of magnitudes "frame *minus* template" obtained by reducing the frame using frame dividing method for two frames of the same field taken at seeing 1."1 and 1."9.

To assess the quality of the photometry of each frame, we plotted the reduced results in the form frame *minus* template magnitudes vs. template magnitudes (this is analogous to the comparison shown in Fig. 3) and graded the plots into six "quality grades". Although this may seem somewhat subjective, we found there was a strong need to classify the frames according to quality to ensure reliable analysis of the resulting stellar photometry. A single parameter such as seeing does not provide a suitable criterion for such a classification. Our grades are much better correlated with the overall errors of the stellar photometry of a given frame. The grades have the following meaning: A – excellent, B – very good, C – good, D – fair, E – lowest acceptable grade, F – not acceptable.

Table 5 shows the correlation of these grades with the corresponding distribution of photometric errors in *I* filter. For grades A – C, the standard deviation in magnitudes per magnitude bin is listed over the full range of observed magnitudes. The numbers are given for three cases of the field density: a) BWC (extremely crowded), b) BW3 (moderately crowded, but the least crowded field in the Baade's Window), c) TP8 (relatively – in Bulge meaning – uncrowded). Only frames of grades A – E were used to construct the final database *i.e.* about 80% of all collected frames.

Table 5

Distribution of Photometric Errors for *I* Filter.

BWC									
	14. ^m 5	15. ^m 0	15. ^m 5	16. ^m 0	16. ^m 5	17. ^m 0	17. ^m 5	18. ^m 0	18. ^m 5
A	0.015	0.018	0.018	0.021	0.025	0.032	0.043	0.063	0.078
B	0.017	0.019	0.022	0.026	0.035	0.047	0.070	0.082	0.098
C	0.020	0.023	0.025	0.030	0.046	0.057	0.094	0.109	0.128
BW3									
	14. ^m 5	15. ^m 0	15. ^m 5	16. ^m 0	16. ^m 5	17. ^m 0	17. ^m 5	18. ^m 0	18. ^m 5
A	0.012	0.013	0.013	0.015	0.019	0.026	0.038	0.053	0.067
B	0.018	0.020	0.022	0.029	0.037	0.048	0.069	0.088	0.106
C	0.019	0.021	0.024	0.035	0.041	0.062	0.088	0.114	0.134
TP8									
	14. ^m 5	15. ^m 0	15. ^m 5	16. ^m 0	16. ^m 5	17. ^m 0	17. ^m 5	18. ^m 0	18. ^m 5
A	0.007	0.010	0.010	0.013	0.017	0.021	0.028	0.039	0.052
B	0.010	0.014	0.015	0.017	0.022	0.028	0.035	0.048	0.067
C	0.013	0.017	0.017	0.019	0.025	0.034	0.041	0.054	0.076

Table 6 contains a summary of the properties of our observations of the Galactic Bulge during 1992. In addition to the total number of frames, the number of frames of each grade is also listed for each field. A complete log of all the observations that includes the exposure times, airmasses, stellar FWHMs, and grades is listed in Table 7. The contents of this table as well as Table 3 (log of clusters of galaxies observations) are also available in digital form from the Acta Astronomica Archive, accessible via INTERNET (see cover page) from the account: */acta/1992/uda_253*.

Table 6

Total Number of Collected Frames.

Field	Filter I						Short exp.	Total	Total OK (ABCDE)	Total Best ABC
	A	B	C	D	E	F				
BW1	27	10	8	1	5	10	3	64	51	45
BW2	17	8	8	1	5	14	2	55	39	33
BW3	22	17	10	2	0	11	2	64	51	49
BW4	14	8	6	4	9	10	1	52	41	28
BW5	22	10	4	1	5	3	2	47	42	36
BW6	15	6	5	4	4	7	2	43	34	26
BW7	21	4	6	4	2	2	1	40	37	31
BW8	10	5	5	5	5	7	1	38	30	20
BWC	28	8	6	3	7	17	3	72	52	42
TP8	12	12	12	0	2	6	1	45	38	36
MM5-A	16	11	3	5	0	11	1	47	35	30
MM5-B	25	5	5	5	3	3	1	47	43	35
MM7-A	11	2	4	1	3	7	2	30	21	17
MM7-B	16	3	4	3	1	2	2	31	27	23

Field	Filter V						Short exp.	Total	Total OK (ABCDE)	Total Best ABC
	A	B	C	D	E	F				
BW1	3	1	3	2	1	2	1	13	10	7
BW2	4	3	1	1	1	2	1	13	10	8
BW3	3	1	4	3	1	1	1	14	12	8
BW4	4	1	4	0	3	1	1	14	12	9
BW5	2	2	0	1	0	0	1	6	5	4
BW6	3	0	1	0	1	0	1	6	5	4
BW7	4	0	1	0	0	0	1	6	5	5
BW8	2	1	1	1	0	0	1	6	5	4
BWC	4	0	1	1	1	2	1	10	7	5
TP8	2	0	0	0	2	2	1	7	4	2
MM5-A	5	3	6	1	0	1	1	17	15	14
MM5-B	4	5	4	1	1	0	0	15	15	13
MM7-A	5	2	1	0	1	1	1	11	9	8
MM7-B	4	0	1	3	0	5	1	14	8	5

Table 7
Log of the Galactic Bulge Observations.

Frame	Middle of Exposure JD-2448000	Exp. (sec)	Field	Filter	Air Mass	Seeing FWHM (pix)	Grade
mr1009	725.74873	600	MMS-A	V	1.306	2.45	C
mr1010	725.76030	480	MMS-A	J	1.246	2.46	A
mr1011	725.76891	480	MMS-B	J	1.207	2.53	A
mr1012	725.78160	600	MMS-B	V	1.158	2.66	D
mr1013	725.79220	600	BW1	V	1.160	2.74	F
mr1014	725.80092	480	BW1	J	1.130	2.68	A
mr1015	725.80999	480	BW2	J	1.102	2.60	B
mr1016	725.81942	600	BW2	V	1.078	2.62	A
mr1017	725.82976	600	BW3	V	1.058	2.47	F
mr1018	725.83943	480	BW3	J	1.041	2.74	B
mr1019	725.84796	480	BW4	J	1.028	2.63	B
mr1020	725.85691	600	BW4	V	1.018	2.58	A
mr1021	725.86749	600	BL1-A	V	1.011	2.49	-
mr1022	725.87645	480	BL1-A	J	1.005	2.49	-
mr1023	725.88490	480	BL1-B	J	1.002	2.52	-
mr1024	725.89348	600	BL1-B	V	1.001	2.34	-
mr1025	725.90364	600	MM7-A	V	1.003	2.23	E
mr1026	725.91196	480	MM7-A	J	1.006	2.55	A
mr1027	726.76161	600	MMS-A	V	1.228	3.39	C
mr1028	726.77125	480	MMS-A	J	1.187	3.05	C
mr1041	726.80049	600	MM7-A	V	1.149	3.57	C
mr1042	726.80907	480	MM7-A	J	1.120	2.98	C
mr1043	726.81826	480	BW4	J	1.078	3.07	B
mr1044	726.82672	600	BW4	V	1.059	3.32	E
mr1045	726.83803	600	BW2	V	1.037	3.47	F
mr1046	726.84657	480	BW2	J	1.025	2.88	C
mr1047	726.85585	480	BW1	J	1.015	2.91	B
mr1048	726.86435	600	BW1	V	1.008	3.03	F
mr1049	726.87704	600	BW3	V	1.002	2.98	D
mr1050	726.88563	480	BW3	J	1.000	2.83	B
mr1051	726.89424	480	BL1-A	J	1.001	2.61	-
mr1052	726.90302	600	BL1-A	V	1.003	2.70	-
mr1053	726.91440	600	BL1-B	V	1.009	2.80	-
mr1054	726.92274	480	BL1-B	J	1.015	2.77	-
mr1077	727.72439	480	MMS-B	J	1.429	3.74	F
mr1078	727.73279	600	MMS-B	V	1.371	2.67	A
mr1079	727.75238	600	MM7-B	V	1.389	2.99	D
mr1080	727.76077	480	MM7-B	J	1.332	2.94	A
mr1081	727.77117	480	MMS-A	J	1.177	2.74	B
mr1082	727.77999	600	MMS-A	V	1.146	2.46	A
mr1083	727.78930	600	MM7-A	V	1.182	2.57	A
mr1084	727.79779	480	MM7-A	J	1.149	2.88	E
mr1086	727.82063	600	BL1-A	V	1.072	2.74	-
mr1087	727.82879	480	BL1-A	J	1.055	2.42	-
mr1088	727.83855	480	BW1	J	1.032	2.78	C
mr1089	727.84761	600	BW1	V	1.020	2.51	A
mr1090	727.85754	600	BW3	V	1.012	2.85	B
mr1091	727.86596	480	BW3	J	1.006	2.88	B
mr1092	727.87434	480	BW2	J	1.002	2.86	E
mr1093	727.88351	600	BW2	V	1.000	2.66	B
mr1094	727.89478	600	BW4	V	1.001	2.52	A
mr1095	727.90390	480	BW4	J	1.005	2.59	C
mr1096	727.91261	480	BW3	J	1.011	2.88	B
mr1113	728.73106	600	MMS-A	V	1.365	2.43	A
mr1114	728.73971	480	MMS-A	J	1.312	2.71	B
mr1115	728.75252	480	MMS-B	J	1.245	2.35	A
mr1116	728.76129	600	MMS-B	V	1.206	2.37	A
mr1117	728.77125	600	MM7-B	V	1.256	2.86	D
mr1118	728.78006	480	MM7-B	J	1.213	2.45	A
mr1119	728.78953	480	BL1-B	J	1.156	2.43	-
mr1120	728.79797	600	BL1-B	V	1.128	2.76	-
mr1121	728.81378	600	BW3	V	1.076	2.25	A
mr1122	728.82268	480	BW3	J	1.057	2.54	A
mr1123	728.83139	480	BW1	J	1.039	2.40	A
mr1124	728.84013	600	BW1	V	1.026	2.23	A
mr1125	728.85033	600	BW2	V	1.015	2.66	C
mr1126	728.85863	480	BW2	J	1.008	2.59	B
mr1127	728.86821	480	BW4	J	1.003	2.48	C
mr1128	728.87781	600	BW4	V	1.000	2.62	E
mr1129	728.88815	600	BL1-A	V	1.001	2.94	-
mr1130	728.89690	480	BL1-A	J	1.003	2.60	-
mr1131	728.90686	600	MM7-A	V	1.008	2.48	A
mr1132	728.91600	480	MM7-A	J	1.015	2.86	A
mr1134	730.76764	600	MMS-B	V	1.161	3.20	B
mr1135	730.77709	600	MM7-B	V	1.203	3.27	F
mr1136	730.79480	480	MM7-B	J	1.134	3.41	D
mr1137	730.80391	480	BL1-B	J	1.095	3.87	-
mr1138	730.81382	600	BL1-B	V	1.071	3.54	-
mr1139	730.79580	600	BW4	V	1.109	3.75	F
mr1140	730.83319	480	BW4	J	1.030	3.07	E
mr1141	730.84233	480	BW2	J	1.018	3.57	E
mr1142	730.83746	600	BW2	V	1.023	3.65	F
mr1143	730.86274	600	BW3	V	1.004	3.58	E
mr1144	730.87169	480	BW3	J	1.001	3.74	F
mr1145	730.88060	480	BW1	J	1.000	3.38	F
mr1146	730.88911	600	BW1	V	1.003	3.33	E

Table 7
continued

Frame	Middle of Exposure JD-2448000	Exp. (sec)	Field	Filter	Air Mass	Seeing FWHM (pix)	Grade
mr1147	730.89983	600	BL1-A	V	1.006	3.76	-
mr1148	730.90877	480	BL1-A	J	1.013	3.18	-
mr1149	730.91916	480	MMS-B	J	1.047	2.91	A
mr1168	731.73572	480	MMS-A	J	1.290	3.58	F
mr1169	731.74415	600	MMS-A	V	1.247	4.13	F
mr1170	731.75470	600	MMS-B	V	1.200	3.30	B
mr1171	731.76308	480	MMS-B	J	1.168	3.48	E
mr1172	731.77127	480	MM7-B	J	1.217	3.30	C
mr1173	731.77973	600	MM7-B	V	1.180	3.70	F
mr1174	731.78984	600	BL1-A	V	1.126	3.44	-
mr1175	731.79875	480	BL1-A	J	1.100	2.90	-
mr1176	731.80751	480	BW1	J	1.069	3.00	B
mr1177	731.81592	600	BW1	V	1.052	2.97	B
mr1178	731.82560	600	BW2	V	1.036	3.50	D
mr1179	731.83426	480	BW2	J	1.024	3.45	F
mr1180	731.84236	480	BW3	J	1.016	3.10	B
mr1181	731.85076	600	BW3	V	1.009	3.22	C
mr1182	731.86023	600	BW4	V	1.003	3.00	C
mr1183	731.86851	480	BW4	J	1.001	2.98	E
mr1184	731.88078	480	BWC	J	1.001	3.11	D
mr1185	731.88908	600	BWC	V	1.003	3.50	F
mr1186	731.90058	600	MM7-A	V	1.009	3.39	A
mr1187	731.91028	600	BL1-B	V	1.016	3.67	-
mr1188	731.91923	480	BL1-B	J	1.026	3.27	-
mr1207	732.71450	600	MM7-B	V	1.611	3.41	F
mr1208	732.72303	480	MM7-B	J	1.505	2.77	A
mr1209	732.73402	480	BL1-B	J	1.387	2.57	-
mr1210	732.74292	600	BL1-B	V	1.328	3.07	-
mr1211	732.75380	600	MMS-B	V	1.193	2.82	A
mr1212	732.76240	480	MMS-B	J	1.161	2.94	B
mr1213	732.77111	480	BW3	J	1.174	3.05	C
mr1214	732.78037	600	BW3	V	1.140	3.04	C
mr1215	732.79076	600	BW1	V	1.105	2.66	A
mr1216	732.79925	480	BW1	J	1.082	3.17	F
mr1217	732.80854	480	MMS-A	J	1.046	2.77	B
mr1218	732.81722	600	MMS-A	V	1.033	2.99	C
mr1219	732.82777	600	BW2	V	1.029	2.83	A
mr1220	732.83652	480	BW2	J	1.018	3.12	E
mr1221	732.84538	480	BWC	J	1.011	2.72	C
mr1222	732.85395	600	BWC	V	1.005	2.98	C
mr1223	732.86401	600	BW4	V	1.001	2.67	C
mr1224	732.87267	480	BW4	J	1.000	2.67	C
mr1225	732.88205	480	BL1-A	J	1.001	2.57	-
mr1226	732.89055	600	BL1-A	V	1.004	2.70	-
mr1227	732.90155	600	MM7-B	V	1.011	2.64	A
mr1228	732.91010	480	MM7-B	J	1.019	2.44	A
mr1229	732.91860	480	BW3	J	1.033	2.37	A
mr1269	734.79054	420	BW4	V	1.094	2.50	E
mr1270	734.80114	421	BW4	J	1.069	2.40	E
mr1287	749.68637	480	BW2	J	1.375	3.89	F
mr1288	749.69486	480	BW4	J	1.330	3.09	F
mr1289	749.70323	480	BW3	J	1.280	3.73	F
mr1290	749.71144	480	BW1	J	1.232	3.40	F
mr1291	749.71985	480	BW3	J	1.199	3.46	F
mr1292	749.73138	480	BWC	J	1.152	3.68	F
mr1293	749.74065	480	BW5	J	1.119	3.41	F
mr1294	749.74967	480	BW7	J	1.097	3.10	F
mr1295	749.76050	480	BW6	J	1.069	3.17	F
mr1296	749.76889	480	BW8	J	1.052	3.21	F
mr1297	749.77888	720	TP8	J	1.052	3.08	B
mr1298	749.79126	481	BW1	J	1.018	3.17	D
mr1299	749.80004	480	BW3	J	1.011	3.17	F
mr1300	749.80824	480	BWC	J	1.005	2.86	E
mr1301	749.81643	480	BW2	J	1.002	3.25	F
mr1302	749.82454	480	BW4	J	1.000	2.92	F
mr1303	749.83268	480	BW5	J	1.001	2.91	E
mr1304	749.84103	480	BW6	J	1.003	2.96	E
mr1305	749.84934	480	BW7	J	1.008	2.72	D
mr1306	749.85934	720	TP8	J	1.010	2.94	B
mr1307	749.87092	480	BW8	J	1.030	3.18	F
mr1308	749.87927	480	BW1	J	1.045	2.76	B
mr1309	749.88736	480	BW3	J	1.057	3.17	C
mr1310	749.89563	480	BWC	J	1.076	3.02	F
mr1311	749.90520	720	BW1	J	1.102	3.04	F
mr1312	749.91456	480	BW2	J	1.130	2.78	C
mr1313	749.92360	720	TP8	J	1.124	2.86	B
mr1314	749.93314	480	BW4	J	1.194	2.99	E

Table 7
continued

Frame	Middle of Exposure JD-2448000	Exp. (sec)	Field	Filter	Air Mass	Seeing FWHM (pix)	Grade
mr1938	810.79090	600	BWC	/	1.312	2.94	D
mr1939	810.80075	600	BW5	/	1.381	3.09	B
mr1940	810.81053	600	BW6	/	1.448	3.09	D
mr1941	810.82001	600	BW7	/	1.525	3.28	C
mr1942	810.82968	600	BW8	/	1.632	3.43	F
mr1943	810.83923	600	TP8	/	1.600	3.53	E
mr1954	811.66419	90	BW1	/	1.001	2.40	-
mr1955	811.67103	90	BW1	/	1.003	2.68	-
mr1956	811.69410	60	BW2	/	1.020	2.42	-
mr1957	811.69704	70	BW3	/	1.022	2.62	-
mr1958	811.70765	800	BW3	/	1.036	2.29	A
mr1959	811.71985	800	BW4	/	1.058	2.33	B
mr1960	811.73179	800	BWC	/	1.086	2.62	B
mr1961	811.73887	90	BWC	/	1.105	2.21	-
mr1962	811.74767	800	MM7-A	/	1.121	2.39	F
mr1963	811.75459	60	MM7-A	/	1.144	2.47	-
mr1964	811.76008	120	MM7-B	/	1.162	2.35	-
mr1965	811.76836	800	BW5	/	1.213	2.66	F
mr1966	811.77532	60	BW5	/	1.246	2.85	-
mr1967	811.78024	100	BW6	/	1.267	2.83	-
mr1968	812.60808	800	MMS-A	/	1.025	2.58	A
mr1969	812.61996	800	MMS-B	/	1.014	2.61	A
mr1970	812.63193	800	BWC	/	1.009	2.39	A
mr1971	812.64387	800	TP8	/	1.009	2.52	A
mr1972	812.65559	800	BW8	/	1.000	2.59	A
mr1973	812.66747	800	BW7	/	1.002	2.51	A
mr1974	812.67932	800	BW6	/	1.009	2.72	A
mr1975	812.69137	800	BW5	/	1.020	3.03	A
mr1976	812.70458	800	BW4	/	1.036	2.71	A
mr1977	812.71713	800	BWC	/	1.059	2.79	A
mr1978	812.72981	800	BW3	/	1.086	2.74	A
mr1979	812.74250	800	BW2	/	1.126	2.93	A
mr1980	812.75567	800	BW1	/	1.172	3.06	A
mr1981	812.76840	800	MM7-A	/	1.211	3.23	D
mr1982	812.78067	800	MM7-B	/	1.268	3.12	A
mr1983	812.80261	800	BWC	/	1.430	3.45	F
mr2003	813.60831	60	BWC	/	1.031	3.10	-
mr2004	813.61359	60	BWC	/	1.024	2.79	-
mr2005	813.61832	60	BW5	/	1.018	3.52	-
mr2006	813.62332	60	BW6	/	1.014	4.32	-
mr2007	813.63172	60	BW7	/	1.008	3.37	-
mr2008	813.63596	60	BW8	/	1.005	3.98	-
mr2009	813.64145	60	TP8	/	1.009	3.51	-
mr2010	813.64562	60	BW1	/	1.001	3.85	-
mr2011	813.64964	60	BW2	/	1.000	4.26	-
mr2012	813.65330	60	BW3	/	1.000	3.52	-
mr2013	813.65696	60	BW4	/	1.000	3.39	-
mr2014	813.66264	60	MMS-A	/	1.011	3.48	-
mr2015	813.66875	61	MMS-B	/	1.016	2.98	-
mr2016	813.67532	60	MM7-A	/	1.006	3.31	-
mr2017	813.67948	60	MM7-B	/	1.008	3.53	-
mr2018	813.69523	240	MM7-B	V	1.022	4.10	-
mr2019	813.70153	240	MM7-A	V	1.031	3.58	-
mr2020	813.70762	240	BW1	V	1.048	3.73	-
mr2021	813.71444	240	BW2	V	1.061	4.22	-
mr2022	813.72025	240	BW3	V	1.070	4.13	-
mr2023	813.72809	240	BW4	V	1.089	4.22	-
mr2024	813.74994	240	BWC	V	1.158	3.32	-
mr2025	813.75515	200	BW5	V	1.181	3.31	-
mr2026	813.76020	180	BW6	V	1.198	3.48	-
mr2027	813.76522	240	BW7	V	1.218	3.42	-
mr2028	813.77064	240	BW8	V	1.247	3.66	-
mr2029	813.77605	240	TP8	V	1.219	3.71	-
mr2030	813.78158	240	MMS-A	V	1.361	3.97	-
mr2089	819.53476	720	MMS-A	/	1.135	2.39	A
mr2090	819.55119	720	MMS-B	/	1.089	2.17	A
mr2091	819.56273	720	MM7-A	/	1.107	2.33	A
mr2092	819.57371	720	MM7-B	/	1.080	2.34	A
mr2093	819.58487	720	BW1	/	1.040	2.23	A
mr2094	819.59589	720	BW2	/	1.025	2.68	A
mr2095	819.60662	720	BW3	/	1.014	2.53	A
mr2096	819.61743	720	BW4	/	1.006	2.33	A
mr2097	819.63115	720	BWC	/	1.001	2.17	A
mr2098	819.64232	720	BW5	/	1.001	2.11	A
mr2099	819.65350	720	BW6	/	1.005	2.63	A
mr2100	819.66458	720	BW7	/	1.011	2.55	A
mr2101	819.67586	720	BW8	/	1.024	2.28	A
mr2102	819.68698	720	TP8	/	1.027	2.26	F
mr2106	821.67308	600	MMS-A	/	1.047	2.54	A
mr2107	821.68295	600	MMS-B	/	1.065	2.47	A
mr2108	821.69322	600	BWC	/	1.061	2.65	A
mr2109	821.70373	600	BW1	/	1.087	2.64	A
mr2110	821.71584	600	BW2	/	1.120	2.35	A
mr2111	821.72565	600	BW3	/	1.148	2.46	A
mr2112	821.73501	600	BWC	/	1.186	2.47	A

Table 7
continued

Frame	Middle of Exposure JD-2448000	Exp. (sec)	Field	Filter	Air Mass	Seeing FWHM (pix)	Grade
mr2113	821.74444	600	BW4	/	1.224	2.47	A
mr2114	821.75368	600	BW5	/	1.278	2.76	A
mr2115	821.76444	660	BW6	/	1.336	3.28	C
mr2116	821.77689	740	BWC	/	1.424	3.28	E
mr2117	821.78800	740	MM7-A	/	1.501	3.51	F
mr2118	821.80083	740	MM7-B	/	1.624	3.87	D
mr2119	821.81478	660	TP8	/	1.663	3.37	C
mr2132	822.48102	800	MMS-A	V	1.338	3.12	B
mr2133	822.49841	660	MMS-A	/	1.244	3.25	F
mr2139	822.53859	660	BW1	/	1.131	2.45	A
mr2140	822.54890	720	BW1	V	1.100	2.36	C
mr2141	822.56200	720	BW2	V	1.068	2.49	B
mr2142	822.57272	660	BW2	/	1.047	2.38	A
mr2143	822.58878	660	BW3	/	1.025	2.46	A
mr2144	822.60180	800	BW3	V	1.011	2.98	A
mr2147	822.62424	720	BW4	/	1.000	3.42	E
mr2148	822.63696	900	BW4	V	1.001	3.33	C
mr2151	822.66211	720	BW5	/	1.018	2.26	A
mr2152	822.67308	800	BW5	V	1.032	2.33	A
mr2153	822.68597	800	BW6	V	1.052	2.58	A
mr2154	822.69693	720	BW6	/	1.075	2.58	A
mr2160	822.73199	720	BW7	/	1.182	2.57	A
mr2161	822.74301	800	BW7	V	1.230	2.78	C
mr2162	822.75545	800	BW8	V	1.300	2.91	C
mr2163	822.76650	720	BW8	/	1.369	3.09	C
mr2164	822.77764	720	TP8	/	1.364	2.99	B
mr2165	822.78849	800	TP8	V	1.442	3.11	E
mr2189	823.53312	720	MMS-A	V	1.107	2.34	C
mr2190	823.54448	600	MMS-A	/	1.079	2.57	A
mr2191	823.55428	600	MMS-B	/	1.059	2.58	A
mr2192	823.56432	720	MMS-B	V	1.042	2.55	B
mr2193	823.57543	720	MM7-A	V	1.051	2.68	A
mr2194	823.58556	600	MM7-A	/	1.034	2.52	A
mr2196	823.61786	720	MM7-B	V	1.004	2.20	A
mr2197	823.62793	600	MM7-B	/	1.002	2.39	A
mr2200	823.64867	600	BWC	/	1.008	2.52	A
mr2201	823.65953	600	BW1	/	1.019	2.26	A
mr2202	823.66964	600	BW2	/	1.031	2.23	A
mr2207	823.69496	600	BW4	/	1.075	2.18	A
mr2208	823.70568	720	BW4	V	1.103	2.13	A
mr2209	823.71652	720	BWC	V	1.138	2.31	A
mr2210	823.72617	600	BWC	/	1.173	2.47	A
mr2211	823.73593	600	BW3	/	1.210	2.79	B
mr2212	823.74669	820	BW3	V	1.262	2.45	A
mr2213	823.75750	600	BW5	/	1.332	2.60	A
mr2214	823.76914	700	BW6	/	1.406	2.89	A
mr2215	823.78032	700	BW7	/	1.491	2.74	A
mr2216	823.79101	700	BW8	/	1.602	2.76	B
mr2217	823.80212	700	BWC	/	1.729	2.94	B
mr2218	823.81290	700	TP8	/	1.706	2.86	A
mr2237	824.53541	600	MMS-A	/	1.094	2.57	A
mr2238	824.54479	600	MMS-B	/	1.072	2.99	A
mr2239	824.55564	600	MM7-A	/	1.089	2.93	A
mr2240	824.56659	600	MM7-B	/	1.065	2.93	A
mr2241	824.58115	600	BW1	/	1.026	2.61	A
mr2242	824.59161	600	BWC	/	1.015	2.70	A
mr2243	824.60099	600	BW2	/	1.007	2.47	A
mr2244	824.61033	600	BW3	/	1.003	3.00	B
mr2245	824.61947	600	BW4	/	1.000	2.46	A
mr2246	824.62897	600	BW5	/	1.001	2.62	A
mr2247	824.63829	600	BW6	/	1.004	2.61	A
mr2248	824.64734	600	BWC	/	1.009	2.82	A
mr2249	824.65657	600	BW7	/	1.017	2.69	A
mr2250	824.66653	600	BW8	/	1.030	2.45	A
mr2251	824.67653	600	TP8	/	1.031	2.42	A
mr2252	824.68626	600	BW1	/	1.065	2.42	A
mr2254	824.70604	600	BW3	/	1.111	3.21	C
mr2255	824.71639	600	BWC	/	1.147	2.63	A
mr2256	824.72756	600	BW2	/	1.192	2.90	A
mr2257	824.73792	600	BW4	/	1.233	2.83	A
mr2258	824.75135	600	BW7	/	1.303	2.86	A
mr2259	824.76092	600	BW5	/	1.373	2.85	A
mr2260	824.77210	600	BWC	/	1.451	3.49	F
mr2261	824.78225	720	BW6	/	1.539	3.34	E
mr2262	824.79382	720	BW8	/	1.664	3.40	E
mr2263	824.80495	720	TP8	/	1.646	3.39	B
mr2276	825.48643	600	MMS-A	/	1.261	3.50	F
mr2277	825.49712	850	MMS-B	/	1.212	3.51	B
mr2278	825.51150	850	MM7-A	/	1.241	2.99	A
mr2279							

Table 7
continued

Frame	Middle of Exposure JD-2448000	Exp. (sec)	Field	Filter	Air Mass	Seeing FWHM (pix)	Grade
mr2285	825.59444	720	BW5	I	1.009	2.50	A
mr2286	825.60574	720	BW6	I	1.003	2.63	A
mr2287	825.61669	720	BW7	I	1.000	2.46	A
mr2288	825.62836	720	BW8	I	1.001	2.54	A
mr2289	825.64388	720	TP8	I	1.005	2.49	A
mr2290	825.65461	600	MMS-A	I	1.036	2.66	A
mr2291	825.66467	600	MMS-B	I	1.052	2.45	A
mr2292	825.67485	600	MM7-A	I	1.041	2.51	A
mr2293	825.68481	660	BWC	I	1.067	2.65	A
mr2294	825.69546	800	BWC	V	1.092	3.23	F
mr2295	825.70752	660	MM7-B	I	1.115	2.86	A
mr2296	825.71772	709	BW1	I	1.165	2.72	A
mr2297	825.72874	660	BW2	I	1.209	3.00	B
mr2298	825.73875	660	BW3	I	1.250	2.98	A
mr2299	825.74899	720	BW4	I	1.307	2.94	B
mr2300	825.76006	720	BWC	I	1.381	2.95	B
mr2301	825.77194	720	BW5	I	1.479	3.34	B
mr2302	825.78324	800	BW6	I	1.576	3.57	F
mr2303	825.79492	800	BW7	I	1.700	3.73	E
mr2304	825.80573	600	TP8	I	1.687	3.71	F
mr2320	826.52962	800	MMS-A	I	1.094	3.60	F
mr2321	826.54936	800	MMS-B	I	1.053	3.55	D
mr2322	826.56515	800	BW1	I	1.041	3.21	C
mr2323	826.57863	800	BW2	I	1.022	3.19	C
mr2324	826.59906	900	BW5	I	1.005	3.01	B
mr2325	826.61461	900	BWC	I	1.000	3.15	C
mr2326	826.63359	610	BW7	I	1.004	3.27	C
mr2327	826.66344	900	BW6	I	1.033	3.21	C
mr2329	826.68980	800	BWC	I	1.085	3.15	C
mr2335	827.51511	800	MMS-A	I	1.127	3.52	F
mr2336	827.52676	800	MMS-B	I	1.095	3.57	C
mr2337	827.53978	800	MM7-A	I	1.110	3.09	B
mr2338	827.55164	800	MM7-B	I	1.080	3.20	A
mr2339	827.58056	800	BW1	I	1.017	3.09	A
mr2340	827.59179	720	BW2	I	1.007	3.47	E
mr2341	827.60267	720	BW3	I	1.003	3.02	A
mr2342	827.61349	720	BW4	I	1.000	2.93	A
mr2343	827.62409	720	BW2	I	1.002	3.11	B
mr2344	827.63476	720	BWC	I	1.006	3.07	B
mr2345	827.64718	720	BW5	I	1.017	3.07	A
mr2346	827.65764	720	BW6	I	1.029	3.02	B
mr2347	827.66838	720	BW7	I	1.044	2.87	A
mr2348	827.67911	720	BW8	I	1.066	2.93	A
mr2349	827.69064	720	TP8	I	1.070	3.18	A
mr2350	827.70119	720	BWC	I	1.124	3.11	C
mr2351	827.72435	720	MMS-A	I	1.257	3.41	F
mr2352	827.73514	720	MMS-B	I	1.314	3.67	D
mr2353	827.75119	720	BW1	I	1.364	3.88	F
mr2369	829.51802	800	MMS-A	I	1.103	3.23	C
mr2370	829.52986	750	MMS-B	I	1.075	3.61	C
mr2371	829.54177	800	MM7-A	I	1.089	3.86	F
mr2372	829.55369	800	MM7-B	I	1.062	3.48	C
mr2373	829.56701	800	BW1	I	1.026	3.32	B
mr2374	829.57998	800	BW2	I	1.012	3.47	F
mr2375	829.59195	800	BW3	I	1.005	3.24	B
mr2376	829.60374	800	BW4	I	1.001	3.21	C
mr2377	829.61636	800	BWC	I	1.001	3.09	A
mr2378	829.62788	800	BW5	I	1.006	3.05	A
mr2379	829.63948	800	BW6	I	1.015	3.05	A
mr2380	829.65112	800	BW7	I	1.027	3.06	A
mr2381	829.66261	800	BW8	I	1.045	2.81	A
mr2382	829.67432	800	TP8	I	1.049	2.66	A
mr2383	829.69006	660	BWC	I	1.108	2.94	A
mr2384	829.69990	660	MMS-A	I	1.175	3.02	B
mr2385	829.70988	660	MMS-B	I	1.216	2.96	A
mr2386	829.72053	700	MM7-A	I	1.207	2.98	A
mr2387	829.73555	720	MM7-B	I	1.279	2.91	A
mr2388	829.74615	720	BW1	I	1.368	3.05	A
mr2389	829.75682	720	BWC	I	1.440	3.09	C
mr2390	829.76776	770	BW5	I	1.562	3.46	C
mr2391	829.78158	770	TP8	I	1.549	3.30	B
mr2408	830.50899	660	MMS-A	V	1.120	2.34	C
mr2409	830.51825	540	MMS-A	I	1.095	2.51	A
mr2410	830.52683	540	MMS-B	I	1.075	2.79	B
mr2411	830.53597	660	MMS-B	V	1.057	2.90	B
mr2412	830.54643	660	MM7-A	V	1.071	3.13	B
mr2413	830.55545	540	MM7-A	I	1.052	3.08	C
mr2414	830.56625	660	MM7-B	I	1.035	3.08	B
mr2415	830.57663	780	MM7-B	V	1.021	3.18	C
mr2416	830.58880	780	BWC	V	1.005	2.79	A
mr2417	830.59949	660	BWC	I	1.001	2.81	A
mr2418	830.60969	660	BW5	I	1.000	2.57	A
mr2419	830.62076	780	BW5	V	1.004	2.80	B
mr2420	830.63305	780	BW6	V	1.011	2.89	A
mr2421	830.64383	660	BW6	I	1.022	2.62	A

Table 7
concluded

Frame	Middle of Exposure JD-2448000	Exp. (sec)	Field	Filter	Air Mass	Seeing FWHM (pix)	Grade
mr2422	830.65470	660	BW7	I	1.036	2.50	A
mr2423	830.66551	780	BW7	V	1.054	2.61	A
mr2424	830.67710	780	BW8	V	1.081	2.64	A
mr2425	830.68787	660	BW8	I	1.109	2.88	B
mr2426	830.69837	660	TP8	I	1.109	2.71	B
mr2427	830.70923	780	TP8	V	1.143	2.63	A
mr2428	830.72114	780	BW1	V	1.239	3.12	C
mr2429	830.73717	660	BW1	I	1.328	3.08	B
mr2430	830.74766	720	BW3	I	1.386	3.27	C
mr2431	830.75832	720	BW4	I	1.471	3.54	E
mr2447	832.48867	660	MMS-A	I	1.168	3.83	F
mr2448	832.50780	840	MMS-B	I	1.108	3.87	E
mr2449	832.52094	840	MM7-A	I	1.125	3.57	F
mr2450	832.53307	840	MM7-B	I	1.091	3.87	E
mr2451	832.54598	840	BWC	I	1.046	3.91	F
mr2452	832.55936	840	BW1	I	1.025	3.38	B
mr2453	832.57176	780	BW2	I	1.012	4.32	F
mr2454	832.58216	499	BW3	I	1.006	4.68	F
mr2458	833.51429	660	BW2	I	1.111	3.26	C
mr2459	833.52484	800	BW2	V	1.083	3.17	B
mr2460	833.53669	800	BW3	V	1.060	3.20	C
mr2461	833.54780	660	BW3	I	1.040	3.26	C
mr2462	833.55867	660	BW4	I	1.024	3.51	F
mr2463	833.56944	800	BW4	V	1.013	3.42	C
mr2464	833.58078	660	BWC	I	1.004	3.30	E
mr2465	833.59081	660	BW5	I	1.001	3.45	C
mr2466	833.60088	660	BW6	I	1.000	3.53	D
mr2467	833.61097	660	BW7	I	1.003	3.46	D
mr2468	833.62087	660	BW8	I	1.008	4.52	F
mr2469	833.63209	660	TP8	I	1.011	3.21	B
mr2470	833.64297	660	BW8	I	1.032	3.57	E
mr2471	833.65288	660	BW1	I	1.049	3.44	C
mr2472	833.66293	660	BWC	I	1.068	3.39	E
mr2473	833.67354	660	MMS-A	I	1.124	3.39	F
mr2474	833.68378	660	MMS-B	I	1.157	3.41	E
mr2475	833.69359	660	MM7-A	I	1.151	3.31	F
mr2476	833.70617	660	MM7-B	I	1.190	3.26	D
mr2477	833.71671	750	BWC	I	1.255	3.31	E
mr2478	833.72832	819	BW5	I	1.324	3.20	A
mr2479	833.73980	700	BW6	I	1.395	3.55	E
mr2480	833.75104	820	BWC	I	1.485	3.51	E
mr2481	833.76407	820	TP8	I	1.492	3.35	C
mr2496	840.48304	660	MMS-A	V	1.114	2.54	A
mr2498	840.52580	660	MMS-B	V	1.030	2.85	A
mr2504	840.56773	770	BWC	I	1.002	2.38	A
mr2505	840.58732	770	BW1	I	1.002	2.53	A
mr2506	840.59912	770	BW2	I	1.007	2.61	A
mr2507	840.61152	770	BW3	I	1.016	2.96	A
mr2508	840.62927	770	BWC	I	1.041	2.68	A
mr2509	840.64108	770	BW4	I	1.061	2.70	A
mr2510	840.65285	770	BW5	I	1.092	2.62	D
mr2511	840.66408	770	BW6	I	1.121	2.56	A
mr2512	840.67527	770	BW5	I	1.162	2.60	A
mr2513	840.68662	770	BW7	I	1.202	2.54	A
mr2514	840.69802	770	BW8	I	1.260	2.65	A
mr2515	840.70901	770	MMS-A	I	1.378	3.14	D
mr2516	840.72672	700	MMS-B	I	1.513	3.40	C
mr2517	840.73790	700	MM7-A	I	1.526	3.24	E
mr2518	840.74847	491	MM7-B	I	1.629	3.63	F
mr2715	845.48105	600	MMS-B	I	1.084	2.82	A
mr2716	845.49533	600	MMS-A	I	1.054	2.58	A
mr2717	845.50476	600	MMS-B	I	1.039	2.47	A
mr2718	845.51422	600	MMS-A	I	1.027	2.68	B
mr2719	845.52382	600	MMS-B	I	1.018	2.53	A
mr2720	845.53341	600	MMS-A	I	1.010	2.60	A
mr2721	845.54294	600	MMS-B	I	1.007	2.44	A
mr2722	845.55243	600	MMS-A	I	1.005	2.68	B
mr2723	845.56174	600	MMS-B	I	1.007	2.66	A
mr2724	845.57126	600	MMS-A	I	1.010	2.64	A
mr2725	845.58071	600	MMS-B	I	1.017	2.65	A
mr2726	845.59080	600	MMS-A	I	1.026	2.51	B
mr2727	845.60010	600	MMS-B	I	1.038	2.62	A
mr2728	845.60970	600	MMS-A	I	1.053	2.73	B
mr2729	845.61909	600	MMS-B	I	1.072	2.63	A
mr2730	845.62873	600	MMS-A	I	1.094	2.76	F
mr2731	845.63992	600	MMS-B	I	1.124	2.65	A
mr2732	845.64933	600	MMS-A	I	1.154	2.85	C
mr2733	845.65905	600	MMS-B	I	1.190	2.85	A
mr2734	845.66950	600					

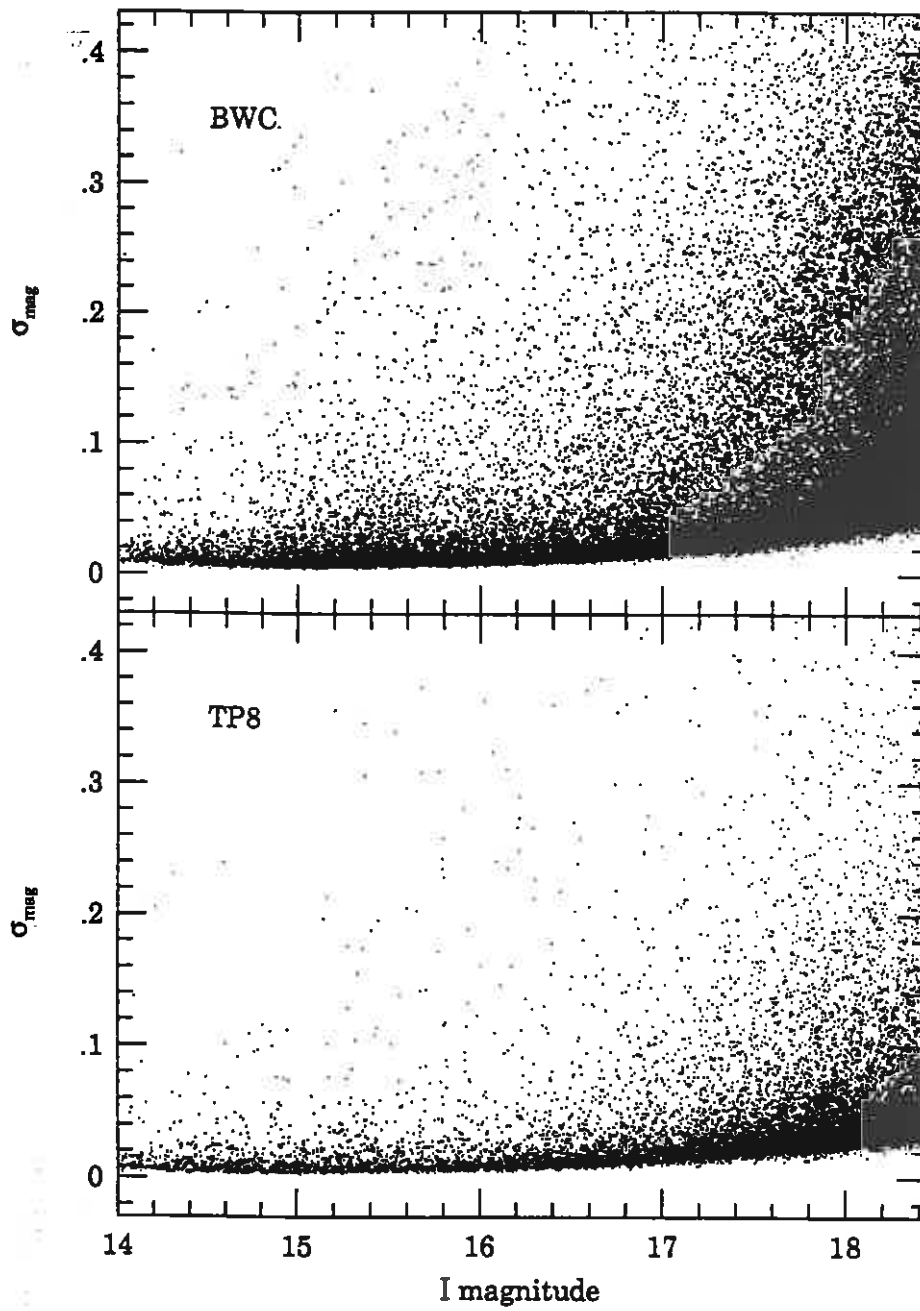


Fig. 4. Standard deviation of magnitude of stars from BWC and TP8 fields.

Fig. 4 is a plot of the standard deviation in the I -band magnitudes vs. I magnitude for the two fields BWC and TP8 (these are the most and least crowded Bulge fields we observed, respectively). The standard deviations were calculated from the all frames with grades A – C included in the databases for these two fields. A strong correlation between the density of the field and the accuracy of the photometry is clearly present. The errors in the photometry of the stars in the TP8 field reach 0.1 mag at brightness approximately 0.6 – 0.8 magnitude fainter than in the BWC field. We found that for frames of the relatively low-density Galactic open cluster Mel 66 obtained with the same telescope and detector, an error 0.1 mag is typically attained at brightness about one magnitude fainter than in even the least crowded Bulge frames for comparable exposure times. Clearly – and not too surprisingly – crowding is the most important limiting factor in our Bulge photometry.

Table 8 lists the approximate numbers of stars detected on BWC, BW3 and TP8 fields. The number of stars with standard deviation less than 0.1 mag is also given. The latter should be suitable for detecting lensing events at the 3σ level of significance.³

Table 8

Number of Detected Stars.

Field	Number of Detected Stars	Number of Stars with $\sigma < 0^m.1$
BWC	250000	70000
BW3	170000	50000
TP8	90000	30000

Fig. 5 shows a number of light curves of some of the variable stars extracted from the databases. Some of these correspond to previously known RR Lyr variables (Blanco 1984); others are newly discovered from our observations. The periods of the latter were found using the Phase Dispersion Minimization Method (Stellingwerf 1978). Zero phase for each star is chosen arbitrary, two cycles are shown for clarity.

³Of course, in a survey as large as ours, 3σ events will actually be rather numerous. Thus, legitimate lensing events must not only be detected, but they must be temporally well-resolved also. This is a much more stringent requirement, and allows lensing events to be confidently identified from repeat observations of even a few million stars.

The project was partly supported through the Polish KBN grant No 2-1173-91-01; through NSF grant AST-9023775 to B. Paczyński, through NASA grant HF-1007.01-90A awarded by STScI which is operated by AURA, Inc. for NASA under contract NAS5-26555 (MM). DoPHOT was written with support from NSF grant AST 83-18504 (Paul Schechter).

REFERENCES

- Blanco, B. M. 1984, *Astron. J.*, **89**, 1836.
 Blanco, B. M. 1992, *Astron. J.*, **103**, 1872.
 Blitz, L., and Spergel, D. N. 1991, *Astrophys. J.*, **370**, 205.
 Gaposchkin, S. 1954, *Var. Star Bull.*, **10**, 337.
 Griest, K. 1991, *Astrophys. J.*, **366**, 412.
 Griest, K., Alcock, C., Axelrod, T. S., Bennett, D. P., Cook, K. H., Freeman, K. C., Park, H.-S., Perlmutter, S., Peterson, B. A., Quinn, P. J., Rodgers, A. W., and Stubbs, C. W. 1991, *Astrophys. J. Letters*, **372**, L79.
 Groth, E. J. 1986, *Astron. J.*, **91**, 1244.
 Landolt, A. U. 1992, *Astron. J.*, **104**, 340.
 Mateo, M., and Schechter, P. 1989, in *The First ESO/ST-ECF Data Analysis Workshop*, eds. P. J. Grosbøl, F. Murtagh, and R. H. Warmels, (Garching: ESO), p. 69.
 Paczyński, B. 1986, *Astrophys. J.*, **304**, 1.
 Paczyński, B. 1991, *Astrophys. J. Letters*, **371**, L63.
 Preston, G. W. 1992, in *Galactic Bulges*, ed. H. Habing. (Dordrecht: Kluwer), in press.
 Stellingwerf, R.F. 1978, *Astrophys. J.*, **224**, 953.
 Terndrup, D. M. 1988, *Astron. J.*, **96**, 884.
 Udalski, A., Szymański, M., Kałużny, J., Kubiak, M., Mateo, M., Preston, G., Krzemiński, W., and Paczyński, B. 1992, in *Galactic Bulges*, ed. H. Habing. (Dordrecht: Kluwer), in press.

This paper is available in the PostScript form from the Acta Astronomica Archive (see cover page) accessible via INTERNET, directory */acta/1992/uda_253*.

FUNDACJA ASTRONOMII POLSKIEJ IM. MIKOŁAJA KOPERNIKA

ACTA ASTRONOMICA
An International Quarterly Journal

Editors

M. KUBIAK and A. UDALSKI

Associate Editor

J. UDALSKA

Address of Editors' Office:

Al. Ujazdowskie 4, 00-478 Warsaw, Poland

FAX: (48-22) 294967

INTERNET: acta@sirius.astro.uw.edu.pl

BITNET: acta@plwauw61.bitnet

Indexed in: Current Contents/Physical, Chemical & Earth Sciences®
Science Citation Index® Research Alert™ Scisearch®

The Acta Astronomica Archive (AAA) can be reached via INTERNET by *anonymous ftp* from the computer [sirius.astro.uw.edu.pl](ftp://sirius.astro.uw.edu.pl) (148.81.8.1). The AAA contains numerical data which the author of the paper wishes to make available for astronomical community (e.g. theoretical models, observations etc.). The data are stored in sub-directories in */acta/year_of_volume/* directory. The names of the sub-directories consist of abbreviation of the last name of the first author followed by number of the starting page of the paper (e.g. */acta/1992/kal.29/*). All files are compressed using *compress* program.

To retrieve a file, *ftp sirius.astro.uw.edu.pl*, give *anonymous* as your user name and your e-mail address as password. Change directory to */acta/...*, set binary mode (command *binary*) and transfer file(s) you are interested in (command *get file_name*). Retrieved file must be uncompressed on your local system using *uncompress* program. Please avoid working hours (8-18) on weekdays for large data transfers.